

**SINGLE-WALLED CARBON NANOTUBE FILM FOR
ELECTROCHEMICAL ENERGY STORAGE DEVICES**

By

Jiepeng Rong

A thesis submitted to the Faculty of the University of Delaware in partial fulfillment
of the requirements for the degree of Master of Science in Mechanical Engineering

Spring 2010

Copyright 2010 Jiepeng Rong
All Rights Reserved

**SINGLE-WALLED CARBON NANOTUBE FILM FOR
ELECTROCHEMICAL ENERGY STORAGE DEVICES**

by
Jiepeng Rong

Approved: _____
Bingqing Wei, Ph.D.
Professor in charge of thesis on behalf of the Advisory Committee

Approved: _____
Anette M. Karlsson, Ph.D.
Chair of the Department of Mechanical Engineering

Approved: _____
Michael J. Chajes, Ph.D.
Dean of the College of Engineering

Approved: _____
Debra Hess Norris, M.S.
Vice Provost for Graduate and Professional Education

ACKNOWLEDGMENTS

It has been a great pleasure for me to study in the University of Delaware in the past two years. I received so much help from the faculty, staff and my friends here, which makes my graduation and this thesis possible.

I would like to firstly convey my deepest appreciation to my advisor and mentor, Dr. Bingqing Wei, who gave me unlimited encouragement, guidance and support in my study and research. There is an old Chinese saying, “Once a teacher, always a father.” Dr. Wei gave me generous tolerance and supports to my craze ideas in research and my life, just like what my father did. Some succeeded, some failed, others, I don’t know. But I am so grateful to him for providing me all those opportunities to explore.

I am most grateful to Dr. Tsu-Wei Chou and Dr. Joshua Hertz for accepting my request to be my thesis committee members. I extend my thanks to Dr. Chaoying Ni, Frank Kriss, Dr. Raul Lobo and Brett Guralnick for helping me in materials characterization during my research here.

I also acknowledge all the staff in the Mechanical Engineering Department, Lisa Katzmire, Letitia Toto, Elizabeth Bonavita and Roger Stahl. They are so nice and helpful since the day I applied to the University of Delaware two years ago. I still remembered that I applied around 15 universities in US. Lisa Katzmire is the only administrative assistant who replied all my request

emails about application progress. It means a lot for an anxious applicant.

Another import set of people to mention are my friends I meet here. Dr. Shinn-Shyong Tzeng, Dr. Charan Masarapu, Dr. Kai-Hshun Huang, Haifeng Zeng, Dr. Wenyan Yin, Xin Li, Qing Zhang, Eric McGinnis, Yang Guan, Xian Xu, Zhixiang Tong all made my research and life easier and more colorful.

I could not have gotten where I am today without the unlimited love and continuous encouragement from my grandmother, my parents, and my girlfriend. I am really blessed to have them.

DEDICATION

To my mother, Xiufen Kong, my father, Youshan Rong, and my girlfriend, Wei Yi.
They make all my efforts meaningful.

TABLE OF CONTENTS

LIST OF FIGURES	viii
ABSTRACT	x
CHAPTER 1. INTRODUCTION	1
1.1 Introduction to Carbon Nanotubes	1
1.2 Carbon Nanotube Macro-Film Synthesis	2
1.3 Introduction to Electrochemical Energy Storage Devices	6
References	8
CHAPTER 2. TANDEM STRUCTURE OF POROUS SILICON FILM ON SINGLE- WALLED CARBON NANOTUBE MACRO FILM FOR LITHIUM-ION BATTERY APPLICATIONS.....	11
2.1 Introduction to Lithium-Ion Battery	11
2.1.1 Significance	11
2.1.2 Working Principles of Lithium-Ion Battery	11
2.1.3 Cathode Materials.....	13
2.1.4 Anode Materials.....	13
2.1.5 Half Cell Configuration	15
2.1.6 Full Cell Configuration	16
2.1.7 Criteria to Evaluate a Lithium-Ion Battery	17
2.2 Literature Review	18
2.3 Experimental Section.....	20
2.3.1 Preparation of SWNT-Cu and Cu Substrates.....	20
2.3.2 Electrodes Preparation and Characterization	20
2.3.3 Cell Assembly and Electrochemical Measurements	21
2.4 Results and Discussion	21
2.4.1 Characterization of As-prepared Samples.....	21
2.4.2 Electrochemical Measurements	25
2.4.3 Structure Change during Charge-Discharge Cycling.....	30
2.5 Conclusions	37
Reference.....	38
CHAPTER 3. STRETCHABLE SUPERCAPACITORS BASED ON BUCKLED SINGLE-WALLED CARBON NANOTUBE MACRO-FILMS	43
3.1 Introduction to Supercapacitor	43
3.1.1 Brief History of Supercapacitor	43
3.1.2 Supercapacitor Operation Principle	44
3.2 Significance	46
3.3 Experimental Section.....	47
3.3.1 Preparation of PDMS Substrate.....	47
3.3.2 Fabrication of Buckled Single-Walled Nanotube Macro-Film on Elastomeric PDMS Substrate.....	48
3.3.3 Supercapacitor Assembly and Electrochemical Measurements	50
3.4 Results and Discussion	51
3.5 Conclusions	54
Reference.....	55
CHAPTER 4. CONCLUSIONS, PUBLICATIONS AND FUTRUE WORK	58

4.1	Conclusions	58
4.2	Publications	59
4.3	Future Work	59

LIST OF FIGURES

Figure 1.1.1	Schematic representation of SWNT	2
Figure 1.2.1	Schematic of CVD furnace	5
Figure 1.2.2	SEM of SWNT macro-film	6
Figure 2.1.2.1	Schematic representative of lithium-ion battery.	12
Figure 2.4.1.1	SEM images of as-prepared Si-Cu sample and Si-SWNT-Cu sample. a, c and e represent top view and cross-section view of the Si-Cu sample in various magnification separately; b, d and f are for the Si-SWNT-Cu sample in corresponding manner. Inset of d shows clearly some cone-shape structures on Si-SWNT-Cu sample are squeezed out due to the internal stress induced during Si deposition. G is X-ray diffraction pattern of Si film on copper foil.	25
Figure 2.4.2.1	a) Comparison of cycling performance of the batteries with Si-Cu, Si-SWNT-Cu and SWNT-Cu samples as electrodes at constant current 0.02C in the first cycle, and 0.1C in the remaining 40 cycles. b) Comparison of Coulombic efficiency of these three electrodes. c) Charge/discharge plots of 1st, 2nd and 41st cycles of Si-Cu. d) Charge/discharge plots of 1st, 2nd and 41st cycles of Si –SWNT-Cu.....	30
Figure 2.4.3.1	SEM images of Si-Cu electrode and Si-SWNT-Cu electrodes after 40 cycles of charge-discharge at 0.1 C rate. (a, c) are the Si-Cu sample. Only minor discontinuous particles are left on the Cu substrate after cycling. (b, d) are the Si-SWNT-Cu sample. The majority of Si film is remained and kept good contact on the Cu substrate through the SWNT film connections after rigorous washing. The uniform domains with porous structures are about 10 microns.	31

Figure 2.4.3.2	Schematic representatives (cross-section view) of structural evolution of Si films upon charge-discharge cycling. Left column is a Si-Cu sample, fabricated by physically depositing Si film directly on a bare copper current collector; right column represents a Si-SWNT-Cu sample with the SWNT macrofilm as a buffer layer between the deposited Si film and the copper current collector. After 40 charge-discharge cycles, the Si film on the bare copper substrate pulverizes severely into discontinuous particles with various sizes and only minority of the Si particles remain on the current collector. The Si film on the SWNT buffer layer becomes a porous structure but hold tightly onto the SWNT film after getting rid of a few cone-shaped Si pieces. The structural difference of the Si film retention can be attributed to the large-specific-surface-area SWNT buffer layer, which is deformable, stretchable and tolerant to the volumetric expansion and shrinkage of Si films due to lithium ions insertion and extraction, compared to the smooth and rigid copper foil.	33
Figure 2.4.3.3	Electrochemical impedance spectroscopy measurements are performed on the cells with Si-Cu sample (a) and Si-CNT-Cu sample (b) separately after the 1st, 3rd, 5th and 10th cycles. The dots in a and b are experimental data, and the lines are curve fitting data with corresponding equivalent circuit in d. Solution Resistance R_c and Charge Transfer Resistance R_{ct} of both Si-Cu and Si-CNT-Cu samples are collected and plotted in c.	37
Figure 3.1.2.1	Schematic representative of electrochemical double layer capacitor	45
Figure 3.3.1.1	The two-electrode supercapacitor setup using a custom made stage favorable for stretching the supercapacitor to a specific length.	48
Figure 3.3.2.1	Fabrication steps of a buckled SWNT macro-film on elastomeric PDMS substrate.....	50
Figure 3.4.1	Cyclic voltammograms of the stretchable supercapacitor measured at 0% and 30% applied strain.	52
Figure 3.4.2	Galvanostatic charge-discharge measurements of stretchable supercapacitor and pristine supercapacitor. (a) illustrates galvanostatic charge-discharge in a constant current density of $1A\ g^{-1}$ with stretchable supercapacitor subjected to different applied strain and pristine supercapacitor. The cycling stability of both supercapacitors is shown in (b).	54

ABSTRACT

Development of materials and structures leading to high energy and power density electrochemical energy storage systems is a major requirement to the power needs of portable electronics and electric vehicles. Lithium-ion batteries and electrical double-layer capacitors are among the leading electrical energy storage technologies today. Carbon nanotubes (CNTs), since the discovery in 1991, have exhibited promising applications in electrochemical energy storage by taking advantage of their unique mechanical, chemical, and electrical properties. Two concrete examples of CNT macro-film's applications in lithium-ion batteries and electrical double-layer capacitors are demonstrated in this thesis.

Lithium-ion batteries with substantially higher specific capacity and better cycling performance are needed in next generation portable electronics, especially if all-electric vehicles are to be deployed broadly as replacements for gasoline-powered vehicles. Silicon (Si) is an attractive anode material being closely scrutinized for use in lithium-ion batteries but suffers from a poor cyclability and early capacity fading. A simple method to fabricate tandem structure of porous Si film on CNT film to significantly improve cycling stability of Si film as lithium-ion battery anode materials was reported in this thesis. With the new structure, both reversible specific capacity and cycling stability of the battery cells are improved. Reversible specific capacity of Si film retains 2221 mAh g⁻¹ after 40 charge-discharge cycles at 0.1C rate, more than 3 times of Si film on regular copper current collector. The enhanced reversible specific capacity was attributed to the unique morphology of CNT film, where the functional mechanism of CNT film was investigated and modeled. The facile method is efficient and effective in improving specific

capacity and stability of Si anode lithium-ion batteries, and will provide a powerful means for the development of lithium-ion batteries.

Supercapacitors, as the complementary energy-storage devices of battery, have been intensively studied due to their longer cycle life and higher specific power density in comparison with batteries. A recent direction in electronic field seeking to develop high-performance circuits to be formed on flexible substrates, namely flexible and stretchable electronics has also attracted considerable attention from scientific and technological communities because of its promising wide applications where flexibility, space savings, or production constraints limit the serviceability of rigid circuit boards or hand wiring. To accommodate the needs of the emerging flexible and stretchable electronics, power source devices like capacitors, which are indispensable components in all electronics, must also be flexible and stretchable in addition to their high energy and power density, light weight, miniaturization in size, and safety requirements. In this thesis, we demonstrated stretchable supercapacitors using buckled single-walled carbon nanotube (SWNT) macro-films as the electrodes and polydimethylsiloxane (PDMS) as the elastomeric substrates. The stretchability depends on the level of pre-stain applied on the PDMS substrate, which could be as high as 30%. The electrochemical performance remains unchanged during mechanical stretch. This stretchable supercapacitor just enlightens a broad area of stretchable energy storage devices, which are naturally compatible with the developed stretchable electronics.

Chapter 1

INTRODUCTION

1.1 Introduction to Carbon Nanotubes

Carbon Nanotubes (CNTs) were discovered by Dr. S. Iijima in 1991 [1]. Fullerenes, as another class of molecules composed entirely of carbon atoms, discovered by Kroto, Smalley and co-workers [2], exist in discrete molecular form and consists of 60 carbon atoms all linked together to form a hollow spherical ball. For planar hexagonal graphite lattice to form into fullerene a positive curvature has to be introduced into the structure. Some of carbon atoms in the lattice arrange themselves to form pentagons to make this possible. From this point of view, a CNT can be regarded as a structure formed by expanding a fullerene molecule with 12 pentagons and millions of hexagons. These hexagon structures are arranged along the wall of the nanotube and the pentagons form the closed structures at the tips of the nanotube. Both CNTs and fullerenes belong to the family of fullerenes, which are defined as any molecules composed entirely of carbon atoms.

Due to their unique one dimensional structures [1, 3], CNTs have long captured the attention of researchers. Their structures allow them to acquire superior electrical, mechanical, chemical and thermal properties [4]. The perfect alignment of the lattice along the tube axis and the closed topology endow nanotubes with in-plane properties such as the electronic structure which is dependent on lattice helicity and elasticity. In addition, the nano-dimensions provide a

large surface area which could be useful in mechanical and chemical applications. Especially, CNT has shown promising applications in electrochemical energy storage devices. Employing CNT-based electrodes in electrochemical devices such as supercapacitors has displayed phenomenal storage capacity [5], compared to conventional capacitors. Rechargeable lithium-ion batteries using CNT electrodes have exhibited 1000 mAh g^{-1} reversible storage capacity, significantly higher than the ideal value of graphite, which is the commercial anode material [6, 7].

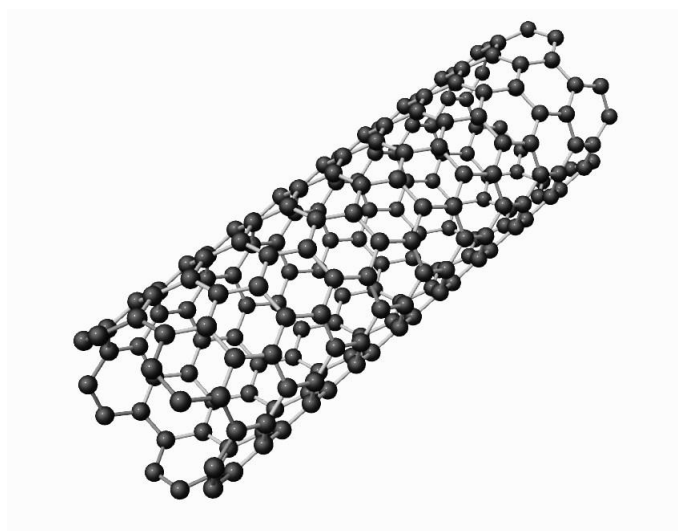


Figure1.1.1 Schematic representation of SWNT

1.2 Carbon Nanotube Macro-Film Synthesis

The ultimate goal of research on CNTs is to make breakthrough that advance nanotechnological applications of bulk nanotube materials. Film-like nanotube macrostructures are drawing great interest because of their unique and usually enhanced properties and tremendous

potential as components in nano-electronic and nano-mechanical device applications or as structural elements in various devices [8, 9]. For example, self-assembled nanotube networks in these films will facilitate the device fabrication process and would provide the opportunities in creating a revolutionary new class of nano devices, especially in energy storage systems where carbonaceous materials electrodes have been commonly used in supercapacitors, lithium-ion batteries and other electrochemical applications [10]. Advantages of considering nanotube films for these applications are their uniform dimensions and large specific surface area. Therefore, a synthetic method that could directly produce a large yield of nanotube macro-films would have a tremendous potential for practical applications in electrochemical energy storage devices.

Motivated by potential applications in electrochemical energy storage devices, our group has succeeded in preparing macro-films of single-walled carbon nanotube (SWNTs) directly on various flexible substrates (copper, stainless steel, aluminum, nickel mesh foils and polymer films) by applying a liquid (solution)-free precursor system, in which ferrocene and sulfur powders were mixed uniformly [11].

SWNT macro-film were grown by a simple floating chemical vapor deposition (CVD) method using ferrocene as carbon feedstock/catalyst and sulfur as an additive to promote SWNT growth to a high percentage. There is no additional carbon source (e.g. xylene, hexane or methane) required for the synthesis. The schematic of the SWNT synthesis setup is shown in Figure 1.2.1. It is an adaption of the CVD technique used previously for the production of SWNTs and essentially a one-step process. In detail, a solid volatile mixture of ferrocene and sulfur (atomic ratio Fe:S=10:1) was introduced into one end of a ceramic tube (total 150 cm in length, 7 cm inner

diameter). An argon flow with rate of 200 mL min^{-1} was then passed through the furnace tube and the furnace was heated to $1100\text{-}1150^\circ\text{C}$. The ceramic tube was moved so as to locate the mixture within the furnace. After 10-30 min reaction duration under a gas flow of argon (1500 mL min^{-1}) and hydrogen (150 mL min^{-1}) mixture, the furnace was allowed to cool down to room temperature.

The as-deposited SWNT film exhibits a perfect structural uniformity and flexibility. Most importantly, the nanotube macro-films could be peeled off from substrates or furnace inner wall and transferred to other substrates without any damage. And the thickness of the films can be controlled in a straightforward manner by controlling the deposition time. Characterizations suggest that the SWNT macro-films are composed of entangled SWNT bundles and a certain amount of impurities, including amorphous carbon and catalytic iron nanoparticles, which could be eliminated by heat treatment and acid wash (heat in air at 450°C for 1 h and rinsing with 37% HCl acid). Figure 1.2.2 shows the purified SWNT film with good structural uniformity.

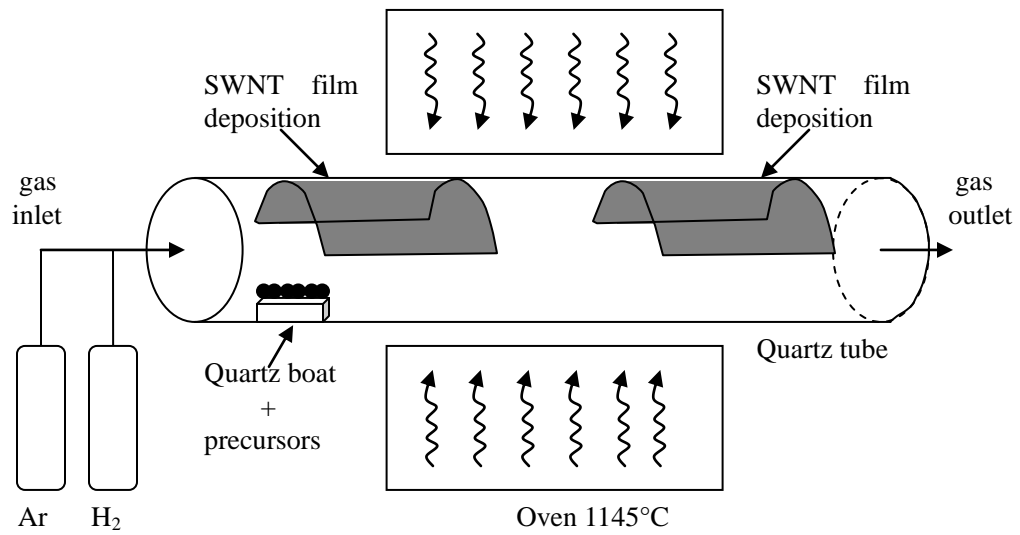


Figure 1.2.1 Schematic of CVD furnace

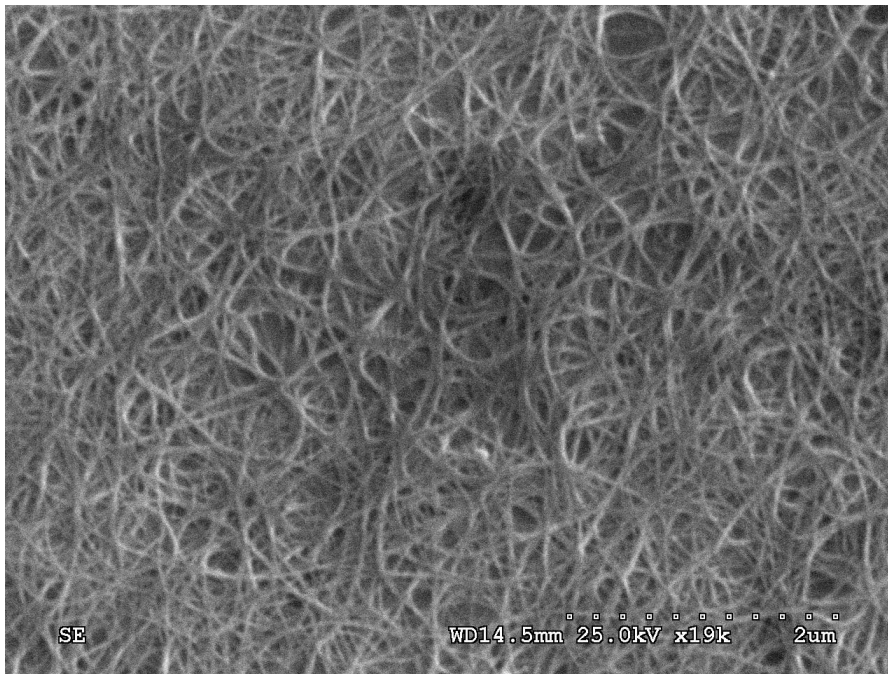


Figure 1.2.2 SEM of SWNT macro-film

1.3 Introduction to Electrochemical Energy Storage Devices

One of the great challenges of the twenty-first century is unquestionably ready availability of cheap energy. According to basic research need for electrical energy storage by Department of Energy, world's energy supply now is primarily from fossil fuels. The energy dilemma facing the world is global warming from CO₂ emissions, mainly generated by internal combustion engine and the combustion of fossil fuels to produce electricity. New technologies for electricity generation from sources that don't produce CO₂, such as solar, wind, and nuclear, together with the advent of plug-in hybrid electric vehicles (PHEV) and even all-electric vehicles (EV), offer the potential of alleviating our present dilemma.

One of the major challenges in realizing this vision is the development of effective electrochemical energy storage systems. Typical electrochemical energy storage devices we have today, such as chemical storage (batteries) or electrochemical capacitors are not capable of meeting energy storage requirements in the future. Portable energy storage devices in the form of rechargeable lithium-ion batteries power the wireless revolution in cellular telephone and laptop computers. These developments have stimulated an international race to achieve the plug in hybrid vehicle (PHEV), which would enable commuters to drive to work under total electric power stored from the grid during the off-peak hours. However, the current battery technology provides only limited vehicle performance and driving range, fewer than 50 miles between charging cycles. Enhanced electrochemical energy storage systems will be needed to make PHEV practical for efficient and reliable transportation.

Electrochemical energy storage technologies will also be critical for effective delivery of electricity generated from solar, wind, and nuclear sources. For example, it would be required to store electricity generated from solar sources for use at night. Because energy use peaks during the day, electricity generated during low-demand periods at nights need to store efficiently for use during peak demand. Electrochemical energy storage devices are also required to smooth short-term fluctuations in power, which is a major problem in the current electrical supply grid. Current energy storage technologies fall far behind these future needs. Without these advanced electrochemical energy storage devices, the goal of non-CO₂ electricity generation will not be realized.

Because the efficient generation and use of non-CO₂ electricity is so important, electrochemical energy storage devices are viewed as the critical technologies needed.

REFERENCES

- 1 S. Iijima, "Helical Microtubules of Graphitic Carbon", *Nature*, vol. 354, pp. 56-58, 1991.
- 2 H. W. Kroto, J. R. Heath, S. C. O'Brien, S. C. Curl, R. E. Smalley, "C-60 Buckminsterfullerene", *Nature*, vol. 318, pp. 162-163, 1985.
- 3 P. M. Ajayan, S. Iijima, "Smallest Carbon Nanotube", *Nature*, vol. 358,

- pp. 23-23, 1992.
- 4 P. M. Ajayan, "Nanotubes from Carbon", *Chemical Reviews*, vol. 99, pp. 1787-1799, 1999.
 - 5 C. Niu, E. K. Sichel, R. Hoch, D. Moy, H. Tennent, "High Power Electrochemical Capacitors Based on Carbon Nanotube Electrodes", *Applied Physics Letters*, vol. 70, pp. 1480-1482, 1997.
 - 6 B. Gao, A. Kleinhammes, X. P. Tang, C. Bower, L. Fleming, Y. Wu, O. Zhou, "Electrochemical Intercalation of Single-Walled Carbon Nanotubes with Lithium", *Chemical Physics Letters*, vol. 307, pp. 153-157, 1999.
 - 7 H. C. Shin, M. Liu, B. Sadandan, A. M. Rao, "Electrochemical Insertion of Lithium into Multi-Walled Carbon Nanotubes Prepared by Catalytic Decomposition", *Journal of Power Sources*, vol. 112, pp. 216-221, 2002.
 - 8 H. W. Zhu, C. L. Xu, D. H. Wu, B. Q. Wei, R. Vajtai, P. M. Ajayan, "Direct Synthesis of Long Single-Walled Carbon Nanotube Strands", *Science*, vol. 296, pp. 884-886, 2002.
 - 9 M. Zhang, S. L. Fang, A. A. Zakhidov, S. B. Lee, A. E. Aliev, C. D. Williams, K. R. Atkinson, R. H. Baughman, "Strong, Transparent, Multifunctional, Carbon Nanotube Sheets", *Science*, vol. 309, pp. 1215-1219, 2005.
 - 10 A. S. Arico, P. Bruce, B. Scrosati, J. M. Tarascon, S. W. Van, "Nanostructured Materials for Advanced Energy Conversion and Storage Devices", *Nature Materials*, vol. 4, pp. 366-377, 2005.
 - 11 H. W. Zhu, B. Q. Wei, "Direct Fabrication of Single-walled Carbon Nanotube Macrofilms on Flexible Substrates", *Chemical Communications*, pp. 3042-3044, 2007.

Chapter 2

TANDEM STRUCTURE OF POROUS SILICON FILM ON SINGLE-WALLED CARBON NANOTUBE MACRO FILM FOR LITHIUM-ION BATTERY APPLICATIONS

2.1 Introduction to Lithium-Ion Battery

2.1.1 Significance

Rechargeable lithium-ion batteries are gaining popularity with the growing demand for portable electronic devices and hybrid vehicles. They are capable of delivering high energy densities and have longer operational life times than many other battery systems [1]. The search for new anode and cathode materials leading to improved electrochemical properties and economical lithium-ion batteries is always demanded.

2.1.2 Working Principles of Lithium-Ion Battery

Rechargeable lithium-ion batteries involve a reversible insertion/extraction of lithium ions into/out of a host matrix which is a lithium insertion compound, during the charge/discharge process. The lithium ions, called the guest species, are generated by the cathode and the host matrix, called the electrode material, is the anode in the lithium-ion battery. Charging process is the insertion of lithium ions into the anode and the discharge process is extraction of lithium ions from the anode. Figure 2.1.2.1 shows the schematic representation of the lithium-ion battery. The cathode and anode are separated using a polymer separator wetted in the electrolyte solution. The electrolyte solution assists in the charge transfer process during the battery charging and

discharging.

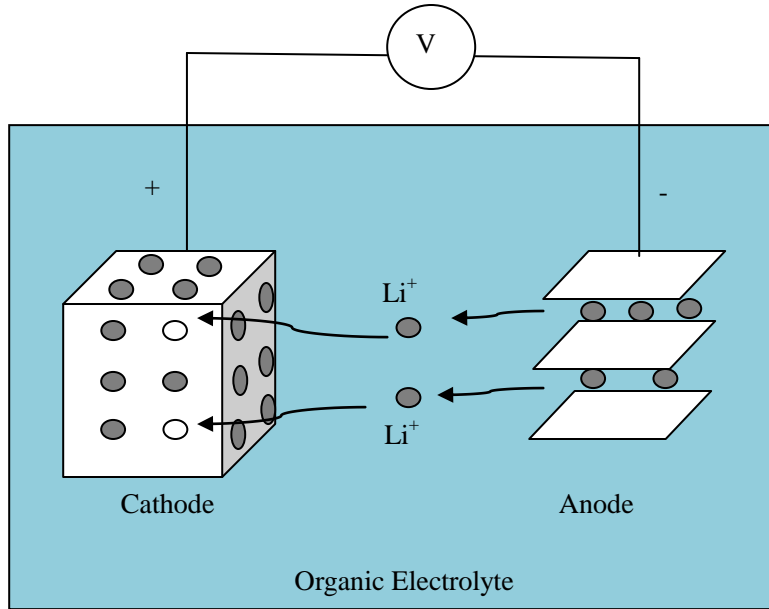


Figure 2.1.2.1 Schematic representative of lithium-ion battery.

The open circuit potential V_{oc} of a lithium-ion cell is given by the difference in the lithium chemical potential between the cathode μ_c and the anode μ_a as

$$V_{oc} = (\mu_c - \mu_a) / F \text{ ----- 2.1}$$

Where F is the Faraday constant. The V_{oc} is determined by the energies involved in both the electron transfer and the lithium ions transfer. While the energy involved in the electron transfer is related to the work functions of the cathode and anode materials, that involved in lithium ions transfer is governed by the crystal structure and the coordination geometry of the site into and from

which the Li^+ ions are inserted and extracted [2].

2.1.3 Cathode Materials

The concept of rechargeable lithium batteries was firstly illustrated with a transition metal sulfide, TiS_2 as the cathode, and the metallic lithium as the anode in a nonaqueous electrolyte [3]. During the discharge process, the lithium ions are inserted into the gaps between the sulfide layers and the charge balance is maintained by the reduction of the Ti^{4+} ions to Ti^{3+} ions. An exact the reverse process occurred during the charge process. Following this demonstration, several other sulfide and chalcogenides were studied as cathodes [4].

However, usage of lithium metal as anode poses several disadvantages. As an alkali metal, lithium is chemically reactive with the non-aqueous electrolyte and results in the formation of a passivating film on the metallic lithium anode. The passivating film leads to a non-uniform plating of lithium during charging and causes total cell failure due to dendritic short circuiting and local over heating [5]. This prompts to pursue a strategy in which the lithium metal is replaced by a lithium insertion compound. Investigations have led to the discovery of several lithium insertion compounds such as LiCoO_2 , LiNiO_2 , LiMn_2O_4 , etc. for usage as cathode materials in lithium-ion cells [6]. These lithium insertion compounds are the sources in the lithium-ion battery that give lithium ions for insertion/extraction into/from the anode materials. Most commercially available lithium batteries currently use LiCoO_2 as the cathode material. Since the cobalt oxide-based cathode is expensive and toxic, a variety of other materials are extensively being studied for possible replacements to make lithium-ion batteries environmentally benign and cost effective.

2.1.4 Anode Materials

Carbon has become the material of choice for anode in the present generation of lithium-ion batteries. The lightweight and low electrochemical potential lying close to that of metallic lithium have made carbon an attractive anode. It has a theoretical capacity of 372 mAh g^{-1} , which corresponds to an insertion of one lithium per six carbon atoms ($x=1$ in Li_xC_6). One of the drawbacks with the carbon anodes is the occurrence of significant amount of irreversible capacity during the first discharge-charge cycle due to unwanted side reaction with electrolyte. More importantly, to meet the increasing energy demand of portable electronic devices and electric vehicles, anode materials of lithium-ion batteries with higher energy density and longer cycle life is needed and increasing efforts have been devoted to its development. Various anode materials such as metal oxides, carbonaceous materials, phosphates, sulfides, etc. have been investigated [7-11].

Of all the family of anode materials studied, silicon (Si) is an attractive anode material for lithium-ion batteries because it has a low discharge potential and the highest known theoretical charge capacity of $4,200 \text{ mAh g}^{-1}$, ten times higher than that of existing graphite anodes and other oxide and nitride materials [12]. However, its applications are much lagged behind due to severe capacity fading caused by early pulverization resulted from up to $\sim 400\%$ volumetric change during insertion and extraction of lithium ions [13-15].

Much effort has been devoted to achieve larger gravimetric capacity and better cyclability on the usage of Si as anode materials in lithium-ion battery. However, either laborious pretreatment or synthesis processes are needed or limited specific energy density is achieved for any reported method (Detailed discussion of previous work could be found in Chapter 2.2 and 2.4.2). One simple method which could be practical for applications and achieve high specific

capacity and good cycling stability is strongly in demand.

2.1.5 Half Cell Configuration

In order to assemble a lithium-ion battery for commercial purpose, it is required to have a complete knowledge of the individual characteristics of the anode and cathode materials and their capabilities to generate or store lithium ions. It is also required to estimate the weights of the cathode and anode materials to assemble an efficient lithium-ion battery. For this purpose, two configurations of lithium-ion battery assembly are typically used, the half cell configuration and the full cell configuration.

A lithium-ion battery in the half cell configuration is generally assembled with an electrode consisting of either the cathode or anode material across metallic lithium. The assembly is very similar as shown in Figure 2.1.2.1. Metallic lithium is the common reference material with either the cathode material or the anode material and always acts as an anode in the half cell. Half cell configuration of lithium-ion battery assembly is used to evaluate the lithium ion generation capability of the cathode material and lithium ion insertion/extraction capability in the anode material.

In case of the half cell study with cathode material such as LiCoO_2 , during the charging process, the lithium ions are generated from LiCoO_2 and get plated onto the metallic lithium. During the discharge process, the lithium ions from the metallic lithium are stripped and sent back to the cathode. In this charge-discharge process, the charging is more important as it depends on the capability of the cathode materials to generate lithium ions. For example, the cathode material LiCoO_2 in the half cell configuration shows a specific capacity of around 100

mAh g^{-1} [16].

When an anode material is being tested in the half cell configuration, during the discharge process, the lithium ions from the lithium metal are stripped and are inserted into the anode. These stored lithium ions in the anode are extracted and plated onto the lithium metal in the charging process. Here both discharge and charge processes are important because they show the ability of the anode material to effectively take and give back the lithium ions. The charging and discharging capacity of the anode material will be generally equal except, in some case such as carbon materials, in the first charge-discharge cycle, the discharge capacity will be much higher than charging [17] due to the electrochemical reactions. The capacity of the anode material to give back the stored lithium ions is called the reversibility of the anode material. In case of carbon anodes, the reversible capacity varies for graphitic carbon and activated carbons depending on their respective structure and morphology [18].

2.1.6 Full Cell Configuration

In the full cell configuration, the electrode with the anode material is assembled across the electrode with the cathode materials. No metallic lithium is used in the full cell configuration. The cathode material in the lithium-ion battery generates lithium ions which get inserted into the anode material during the charging process. The reverse happens during the discharge process. The exact amount of lithium ions that the cathode material generate for a given weight should match the amount of anode material that can store effectively all the generated lithium ions by the cathode.

A lithium-ion battery in the full cell configuration provides the opportunity to test the

battery as a commercial product. Once the respective capacities of the cathode and anode materials are obtained from the half cell configuration testing, the appropriate weight of the cathode and anode materials required for a full cell testing can be calculated. For example, assume that the cathode material LiCoO_2 gave a charge capacity of 100 mAh g^{-1} in the half cell configuration across lithium metal. This means one gram of the cathode material can provide lithium ions pertaining to a maximum of 100 mAh of specific capacity. Similarly, assume that the carbon anode material gives an insertion and extraction charge capacity of 372 mAh g^{-1} in the half cell configuration across lithium. It means one grams of carbon anode can provide a reversible capacity of 372 mAh. Thus, for one gram of graphite anode material considered for the full cell, 3.72 gram of LiCoO_2 cathode material is required for an optimum performance of the lithium-ion battery.

2.1.7 Criteria to Evaluate a Lithium-Ion Battery

The performance of any lithium-ion battery could be evaluated by three parameters, rate capability, specific capacity and cycling life. Generally, we are always looking for electrode materials with high rate capability, high specific capacity, and good cycling life.

The theoretical value of the specific capacity of one material generally tells the maximum charge could be stored in unit-weight electrode material. The actual available capacity depends on the current applied during charge or discharge. Generally speaking, the higher current applied, the lower capacity could be achieved. For example, theoretical specific capacity of graphitic carbon is 372 mAh g^{-1} , meaning that 372 mA current could charge the lithium-ion battery with one gram of graphite material to a full storage in one hour. And if double current is used, usually the battery is fully charged in less than half an hour. Obviously, less than 372 mAh charge is stored in the battery, since constant current is applied.

Lithium-ion batteries are tested by conducting charge-discharge studies at specific current rates such as 0.1 C, 0.5 C, 1 C, etc. The rate capability determines the rate at which the battery can be charged and discharged properly. If a carbon (theoretical specific capacity is 372 mAh g⁻¹) anode based lithium-ion battery is charge-discharged at a constant current of 372 mA g⁻¹, it is known running the battery at 1 C rate. Similarly, if the battery is charged and discharged at a constant current of 37.2 mA per gram of carbon material, then it is called 0.1 C rate. A system with better rate capability signifies a faster charging/discharging, which is an important requirement when lithium-ion batteries are used as power sources for electric vehicle applications.

One full charge and discharge is called one cycle, which is applicable in both lithium-ion battery and electrochemical double-layer capacitor study. Good cycling life means specific capacity of electrode materials keep stable or experience minor degradation during continuous charge and discharge.

2.2 Literature Review

As mentioned in section 2.1.4, Si is an attractive anode material for lithium-ion batteries because it has a low discharge potential and the highest known theoretical charge capacity of 4,200 mAh g⁻¹, ten times higher than that of existing graphite anodes and other oxide and nitride materials. However, its applications are much lagged behind due to severe capacity fading caused by early pulverization resulted from up to ~400% volumetric change during insertion and extraction of lithium ions.

Thus far, it was evidenced that Si nanostructures such as three-dimensional porous Si

particles [19], Si nanocomposites [20], nest-like Si nanospheres [21], Si nanotubes [22], Si core-shell nanowires [23] and amorphous or crystalline Si thin films [24], have shown improved electrochemical performance than the bulk Si material and are considered to be excellent candidates for high performance electrode materials in lithium-ion batteries. Among the various Si nanostructures, film-like Si nanostructures can provide additional advantages, for instance, compatible to traditional battery design, good electrical contact on current collectors, unnecessary binder material reduction, and more importantly, compatible to modern semiconductor techniques for an easy scale-up.

However, studies have proved that the adherence of Si films to current collectors is the key factor that governs the electrochemical performance of the lithium-ion batteries and developing such kind of anodes is very challenging [25-27]. Limited improvements have been reported on cycle stability and cycle life of lithium-ion batteries with Si thin films deposited on current collectors with modified surface by techniques such as chemical etching or electroplating, but at the cost of either laborious pretreatment processes of substrates or decreasing specific energy density [28, 29].

We successfully developed a simple method to employ single-walled carbon nanotube (SWNT) macrofilms [30] as buffer layers between the Si thin films and the current collectors in order to significantly boost the electrochemical performance of lithium-ion batteries. By simply coating a SWNT macrofilm on a regular copper current collector followed by physical deposition of a Si thin film to form a tandem structure, excellent electrochemical performance with a high reversible specific capacity have been achieved. The SWNT macrofilms not only provide

excellent adhesion between the Si film, the SWNT film and the copper substrate proved by SEM observations, galvanostatic charge-discharge cycling, and electrochemical impedance spectroscopy analysis, but also are deformable and stretchable sample holders, which are able to tolerate the drastically volumetric expansion and shrinkage of Si films due to lithium-ion insertion and extraction. In addition, the SWNT macrofilm itself is a good candidate as anode material for lithium-ion batteries; they can easily be transferred to any substrates (such as copper foil) without damage to form extremely strong adhesion between the SWNT film and the current collector, which can withstand ultra-sonication treatment. These unique advantages enable this simple method attractive and practical for applications.

2.3 Experimental Section

2.3.1 Preparation of SWNT-Cu and Cu Substrates

Two kinds of substrates were used for electrode preparation in this study, one was bare copper foil (Cu) and the other was the copper foil coated with SWNT macrofilm buffer layer (SWNT-Cu). Detailed SWNT macrofilm preparation is presented in Chapter 1. As-prepared SWNT film is purified by a combination of oxidations (heat in air at 450 °C for 1h) and rinsing with acid (37% HCl) to remove amorphous carbon and iron particles. The SWNT film could be prepared up to 200 cm² with our facility and could be peeled off, purified, and transferred to other substrates without any damage. After purification, SWNT film is coated on bare copper foil and dried at 100°C in the air. After that, Cu and SWNT-Cu current collector could be simply punched with a hole-puncher in 0.5 inch diameter.

2.3.2 Electrodes Preparation and Characterization

Si thin films were deposited on both substrates in a high-vacuum electron beam evaporation system under 8×10^{-5} Pa. To obtain same thickness of the Si films on these two substrates, the Cu foil and SWNT coated Cu foil were mounted on the substrate holder at the same time and with the same distance of 30 cm to the evaporation source, which is high-purity (99.999%) Si target. The deposition rate (40 nm min^{-1}) and film thickness were controlled by a quartz crystal thickness monitor and a rate controller.

2.3.3 Cell Assembly and Electrochemical Measurements

The as-prepared electrodes were structurally analyzed using scanning electron microscope (SEM) and X-ray diffraction technique (XRD). Electrochemical performance were characterized by assembling two-electrode battery coin cells in argon filled glove box with lithium metal as the reference and the counter electrode in 1M LiPF_6 in EC:DEC electrolyte. Batteries with the Si-Cu anode and the Si-SWNT-Cu anode were characterized separately at 0.05 C in the first cycle and then 0.1 C rate for the subsequent 40 cycles within 3-0.005 V voltage range. For both samples, only Si was considered as the active material for setting current density. The two samples have same Si weight, typically 0.15 mg due to same deposition parameters. After electrochemical measurements, the coin cells were disassembled outside the glove box and washed with ethanol for SEM analysis.

2.4 Results and Discussion

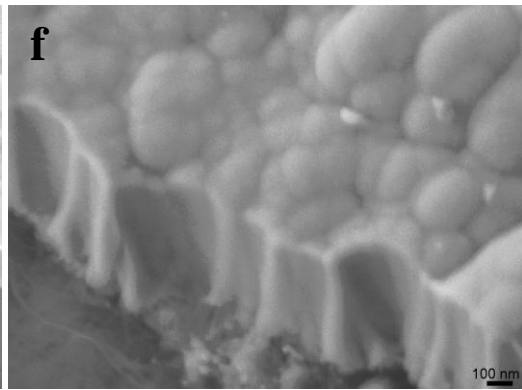
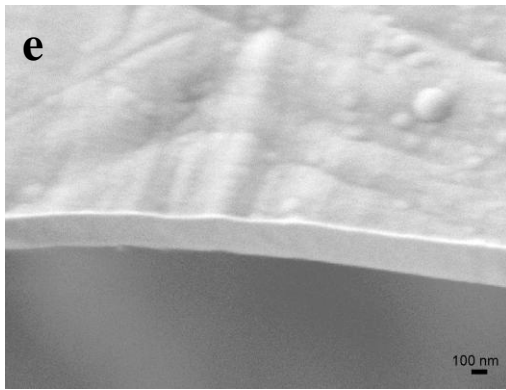
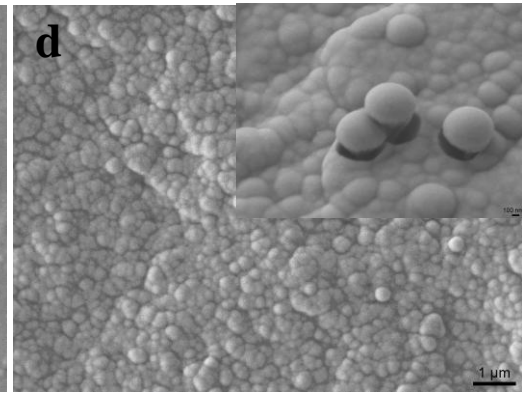
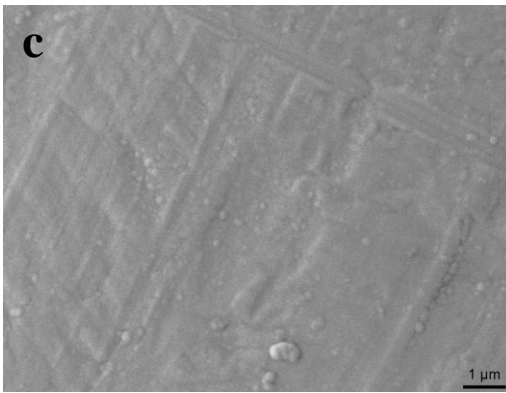
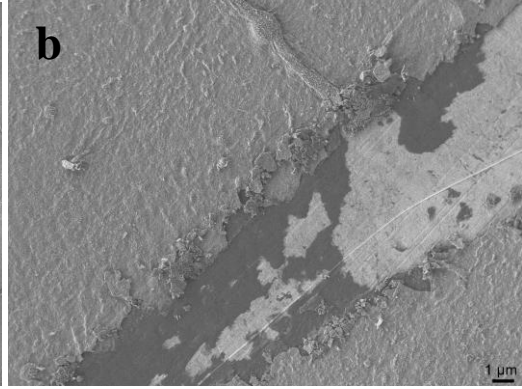
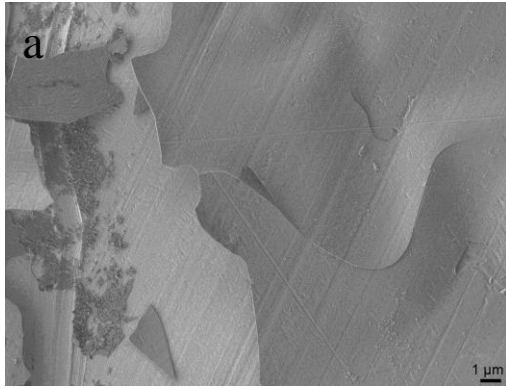
2.4.1 Characterization of As-prepared Samples

An immediate adhesion analysis of Si film on Cu and on SWNT-Cu samples can be simply compared using the scratching method, as shown in Fig. 2.4.1.1 a and b. Under low magnification, we can see cracks in Si film inevitably formed. For those on the bare Cu substrate,

cracks once formed, spread quickly through a large area, and make the whole film into small pieces which lose attachment to the Cu foil substrate (Fig. 2.4.1.1a). While cracks in Si film on the SWNT-Cu foil are quite localized and the majority of the Si film adheres fairly to the SWNT-Cu foil (Fig. 2.4.1.1b). It is plausible that a strong internal stress could easily be formed during the physical deposition on the relatively smooth Cu surface. This can be further confirmed by top views of the samples under a higher magnification, where the Si film on the Cu foil presents relatively smooth and flat surface (Fig 2.4.1.1c). The Si film on the SWNT-Cu substrate, however, has convex morphology with caps of cone-shaped “lattice” through the whole Si film (Fig. 2.4.1.1d). Some cones may be squeezed out to release the internal stress formed during the physical deposition (inset of Fig. 2.4.1.1d). It is interesting to note that similar internal stress induced by lithium-ion insertion into Si is also expected to facilitate some cone-shaped Si “lattice” to be removed in order to provide free space for stress releasing, resulting in porous Si film formation, which is proved by the experimental results.

This unique morphology is attributed to the uneven surface provided by the SWNT macrofilm. It has been recognized that a larger specific interface area would yield a better adhesion between two components [31]. The SWNT macrofilm, formed with tangled SWNT building blocks, provides a rough and large surface with nanosized features [30], which enhance interface adhesion between the Si film and the copper substrate. Meanwhile, the SWNT film facilitates the formation of the cone-shaped structures inside the Si film during physical deposition. These cone-shaped structures allow some “cone-caps” to be easily removed in order to release internal stress, benefiting electrochemical cycling stability as discussed below.

The microstructure difference is also reflected from the cross-section view of these two samples. The Si film on Cu foil exhibits very smooth edge (Fig. 2.4.1.1e) compared to a dental edge of the Si film on SWNT-Cu foil (Fig. 2.4.1.1f), which shows again cone-shaped grains. Both samples employed for electrochemical characterizations have same thickness of ~300 nm (Figs. 2.4.1.1e, 2.4.1.1f). XRD analysis (Fig. 2.4.1.1. g) suggests an amorphous structure (a-Si) of the deposited Si films, no Si reflection peaks were detected except those from the copper substrate by XRD analysis.



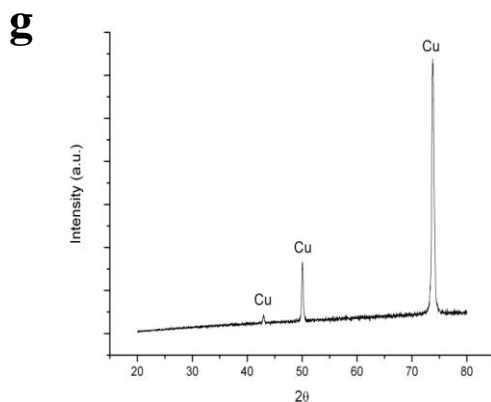


Figure 2.4.1.1 SEM images of as-prepared Si-Cu sample and Si-SWNT-Cu sample. a, c and e represent top view and cross-section view of the Si-Cu sample in various magnification separately; b, d and f are for the Si-SWNT-Cu sample in corresponding manner. Inset of d shows clearly some cone-shape structures on Si-SWNT-Cu sample are squeezed out due to the internal stress induced during Si deposition. G is X-ray diffraction pattern of Si film on copper foil.

2.4.2 Electrochemical Measurements

Galvanostatic charge-discharge cycling stability measurements were carried out with three samples, 300 nm Si film on the bare Cu substrate (Si-Cu), 300 nm Si film on the SWNT film coated Cu substrate (Si-SWNT-Cu), and a pure SWNT film on the bare Cu (SWNT-Cu). For the first two samples, the charge-discharge cycling was conducted at 0.05 C rate for the first cycle and at 0.1 C rate for the subsequent cycles. The charge-discharge current rate was calculated based on the maximum theoretical capacity of Si, i.e. 4200 mAh g⁻¹. The third one, i.e. the SWNT-Cu sample, was a control experiment which can provide contribution portion from SWNT film in the Si-SWNT-Cu electrode. Thus, the same current as used for the first two samples was applied.

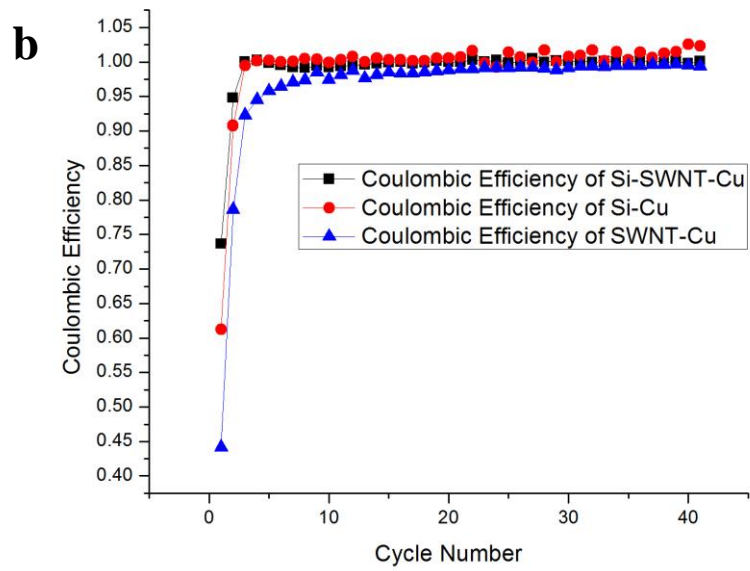
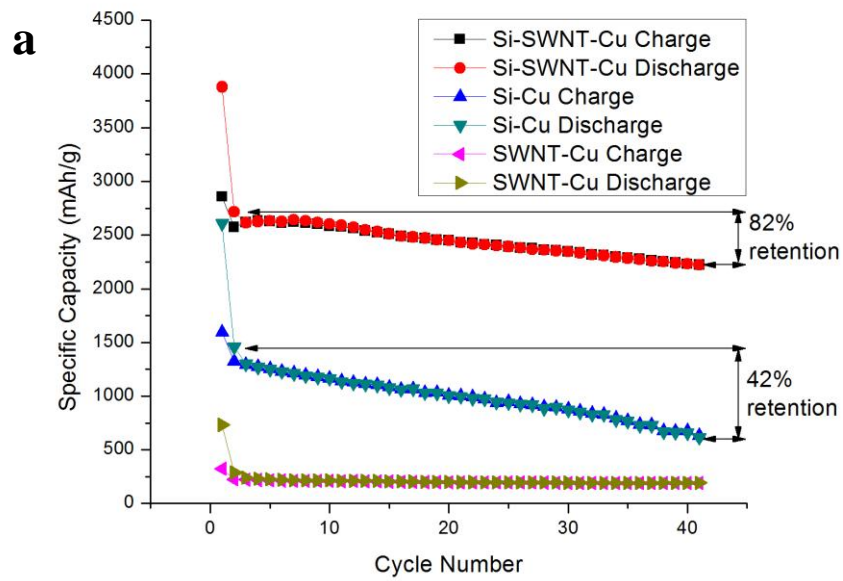
The charge-discharge experimental results (Fig. 2.4.2.1) revealed that the battery cell with Si-SWNT-Cu electrode showed the best electrochemical performance, in terms of both specific capacity and cycling stability compared to that with the Si-Cu electrode, which showed almost linear, sharp decrease during lithium-ion insertion and extraction (Fig. 2.4.2.1a). 1st, 2nd and 41st charge-discharge voltage profiles of both Si-Cu (Fig. 2.4.2.1c) and Si-SWNT-Cu (Fig. 2.4.2.1d) reveal that, after 40 charge-discharge cycles, the specific discharge capacity of the Si-SWNT-Cu cell still retains 2221 mAh g⁻¹, which is about 3.6 times of the Si-Cu cell, and 11.5 times of the pure SWNT film cell. The Si-SWNT-Cu cell exhibited significantly improved capacity retention in comparison with the Si-Cu cell performance. After 40 charge-discharge cycles at 0.1C rate, 82% of the specific discharge capacity is retained for the Si-SWNT-Cu cell, while only 42% percent is retained for the Si-Cu cell (Fig. 2.4.2.1a).

To estimate the capacity contribution from the Si film and from the SWNT film in the tandem structure configuration, battery cell using pure SWNT film as the anode electrode with the same weight as that in the Si-SWNT-Cu sample was characterized by applying the same current density. The cell consisting the pure SWNT film gave 732 mAh g⁻¹, 288 mAh g⁻¹ and 193 mAh g⁻¹ discharge capacity in the 1st, 2nd and 41st cycle (Fig. 2.4.2.1a), which are 18.9%, 10.6% and 8.7% of the discharge capacity of the Si-SWNT-Cu cell in the corresponding cycle, respectively, indicating that Si dominated the capacity contribution in the Si-SWNT-Cu battery cell.

In addition, the tandem structure of the Si film on SWNT film shows a better coulombic efficiency compared to the pure Si film and the pure SWNT film. The pure SWNT cell (SWNT-Cu) has about 44% first cycle coulombic efficiency, indicating as high as more than 50%

irreversibility. The Si film cell (Si-Cu) in this experiment shows 61% first cycle coulombic efficiency, while the tandem structure cell (Si-SWNT-Cu) exhibits the highest first cycle coulombic efficiency of ~74% (Fig. 2.4.2.1b). The high coulombic efficiency of the Si-SWNT-Cu cell may be associated with the tandem structure, where the Si coating layer may decrease the occurrence of side reactions between the SWNT film and the electrolyte by reducing their direct contacts.

Compared to previous efforts to achieve larger gravimetric capacity, higher coulombic efficiency and better cyclability on the usage of Si as anode materials in lithium-ion batteries, which can be categorized as film-like Si anode [29, 32], Si composite anode [20, 33-35] and novel structures of Si anodes (such as nanoparticles, nanowires, nanotubes, nanorods, nest-like nanospheres and three-dimensional porous particles) [19, 21, 22, 36-38], our method has either a superior retention of specific capacity during long cycling or obviously much better labor and cost efficiency. For example, specific capacity of 800 mAh g⁻¹ [29] and about 1000 mAh g⁻¹ specific capacity after 20 cycles [32] have been achieved using the film-like Si anodes; 500 to 1500 mAh g⁻¹ have been observed after 20 cycles using the Si composite anodes [20, 33-35]. As to novel structures of Si, the third category mentioned above, 1000 to 1600 mAh g⁻¹ stable capacity using nanorods [36], nanowires [37] and nanospheres [21] have been observed after 40 charge-discharge cycles. Our experimental results show a better electrochemical performance in terms of both specific capacity and cycling stability. Thus far, better specific capacities with Si nanowires, Si nanotubes and three-dimensional porous nanoparticles have been reported [19, 22, and 38]. However, either chemical vapor deposition to synthesis Si nanowire and nanotubes or sol-gel method and HF etching to form porous nanoparticles are much more laborious and time-consuming processes comparing to this one-step Si physical deposition.



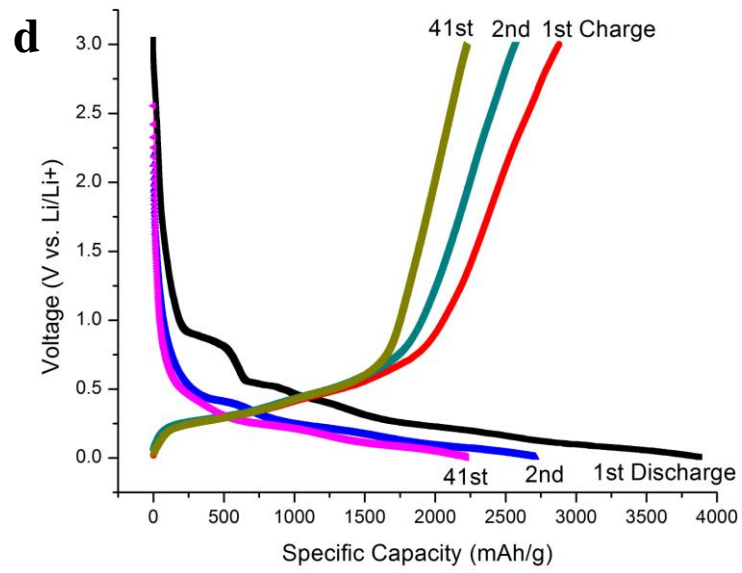
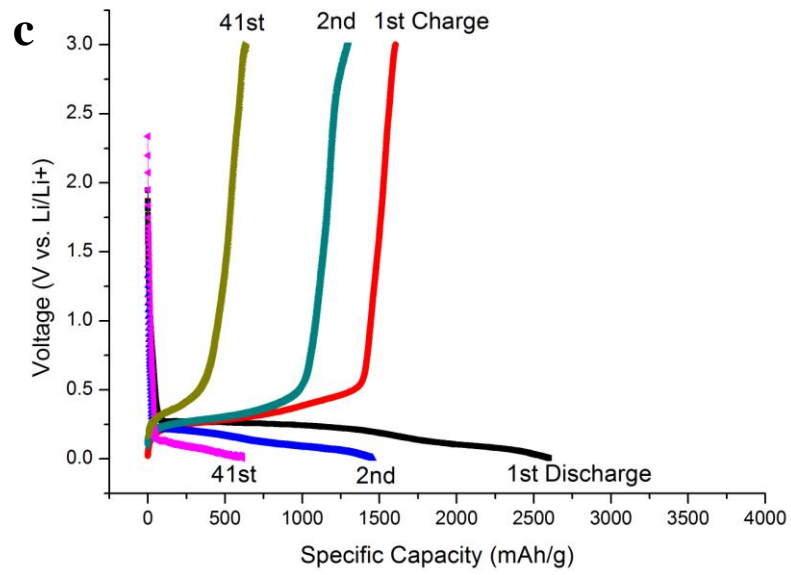


Figure 2.4.2.1 a) Comparison of cycling performance of the batteries with Si-Cu, Si-SWNT-Cu and SWNT-Cu samples as electrodes at constant current 0.02C in the first cycle, and 0.1C in the remaining 40 cycles. b) Comparison of Coulombic efficiency of these three electrodes. c) Charge/discharge plots of 1st, 2nd and 41st cycles of Si-Cu. d) Charge/discharge plots of 1st, 2nd and 41st cycles of Si-SWNT-Cu.

2.4.3 Structure Change during Charge-Discharge Cycling

After 40 charge-discharge cycle at 0.1C rate, the battery cells were disassembled outside the glovebox and the electrodes were washed rigorously with ethanol for structural analysis. SEM observations of the Si-Cu electrode (Figs. 2.4.3.1a, and c) and the Si-SWNT-Cu electrode (Figs. 2.4.3.1 b, and d) after cell disassembling revealed that the Si film on the bare copper substrate pulverized severely after cycling, and only small amount of Si remained to connect to the Cu current collector as discontinuous particles with various sizes (Figs. 2.4.3.1a, and c). However, the Si film was intact on the SWNT film after turning into porous structures. Although the film broke into grain domains with gaps between them after lithiation/delithiation cycles, each grain domain maintained its strong adhesion onto the SWNT film (Figs. 2.4.3.1b, and d) even after rigorous washing. The adhesion of the Si film can be attributed to the large-specific-surface-area SWNT buffer layer, which is deformable, stretchable and tolerant to the volumetric expansion and shrinkage of Si films due to lithium-ion insertion and extraction, compared to the smooth and rigid copper substrate (Figs. 2.4.3.1a, and c).

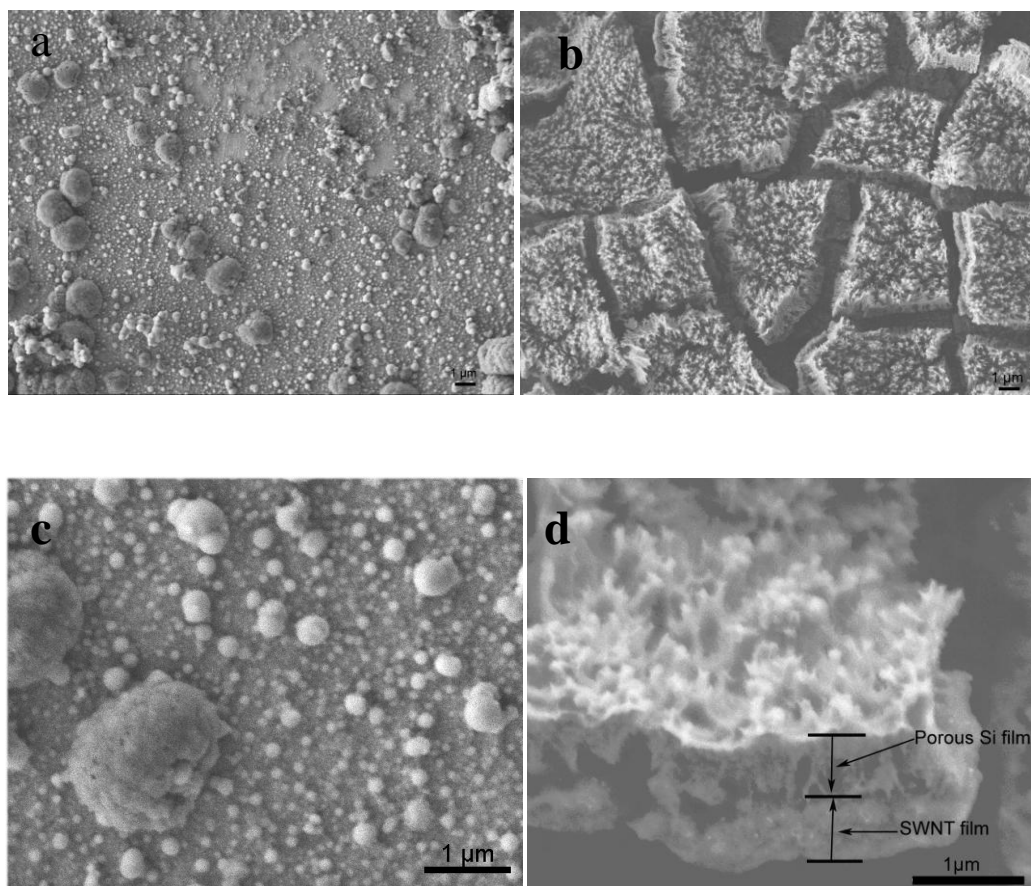


Figure 2.4.3.1 SEM images of Si-Cu electrode and Si-SWNT-Cu electrodes after 40 cycles of charge-discharge at 0.1 C rate. (a, c) are the Si-Cu sample. Only minor discontinuous particles are left on the Cu substrate after cycling. (b, d) are the Si-SWNT-Cu sample. The majority of Si film is remained and kept good contact on the Cu substrate through the SWNT film connections after rigorous washing. The uniform domains with porous structures are about 10 microns.

The structural evolution of Si films upon charge-discharge cycling can be illustrated as Figure 2.4.3.2, where the left panel is the Si-Cu electrode, fabricated by physically depositing Si film directly on a bare copper current collector; while the right panel represents the Si-SWNT-Cu electrode with the SWNT macrofilm as a buffer layer between the deposited Si film and the copper

current collector. The Si film on the bare copper substrate typically has a smooth, uniform and dense layer structure while the Si film on the SWNT film coated substrate exhibits a column or cone-shaped “lattice” structure. During charge-discharge cycling, Si film on Cu would experience a significant volume expansion and pulverize into discontinues particles and only small amounts of Si stay on the current collector after cycling. However, similar internal pressure in Si-SWNT-Cu sample introduced by volumetric change during lithium-ion insertion/extraction can be released by getting rid of some cone-shaped Si grains. The Si film on the SWNT buffer layer, therefore, becomes a porous structure but hold tightly onto the SWNT film. The SWNT film provides deformable and stretchable tolerance to the volumetric expansion and shrinkage of the Si films due to lithium-ion insertion and extraction.

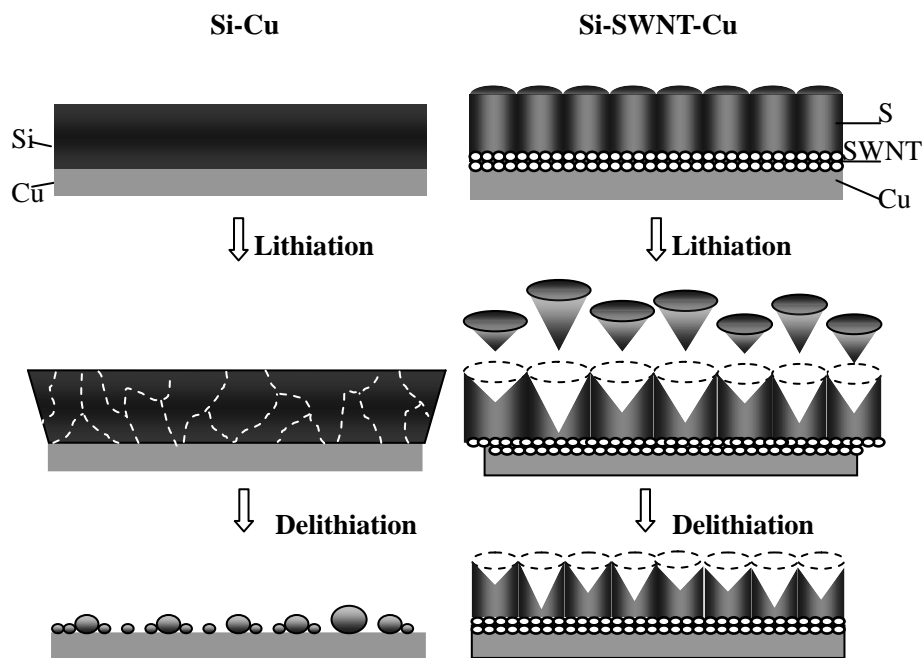
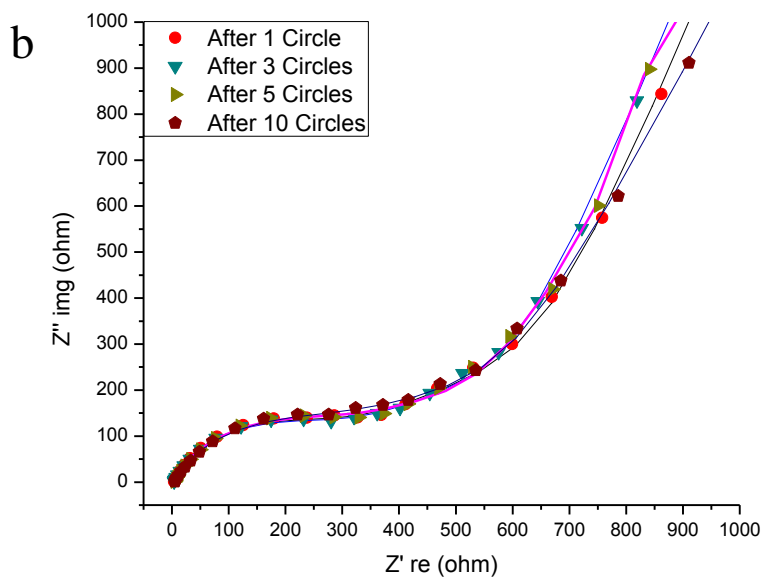
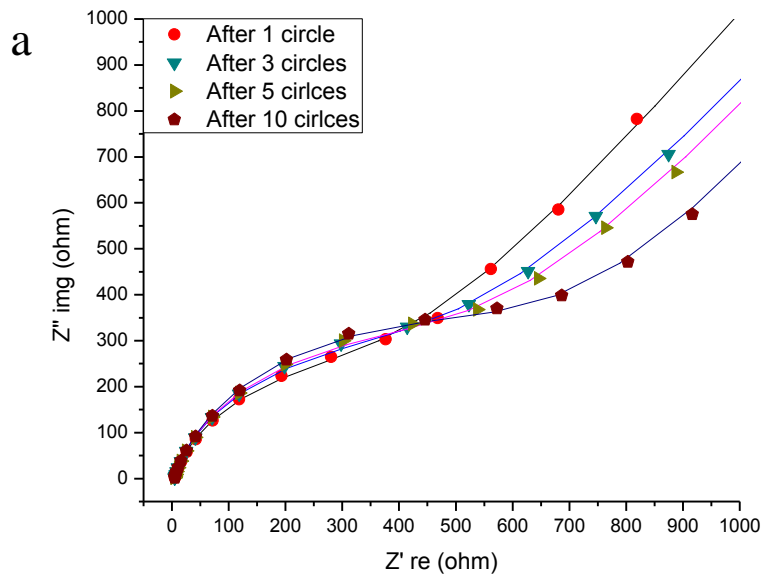


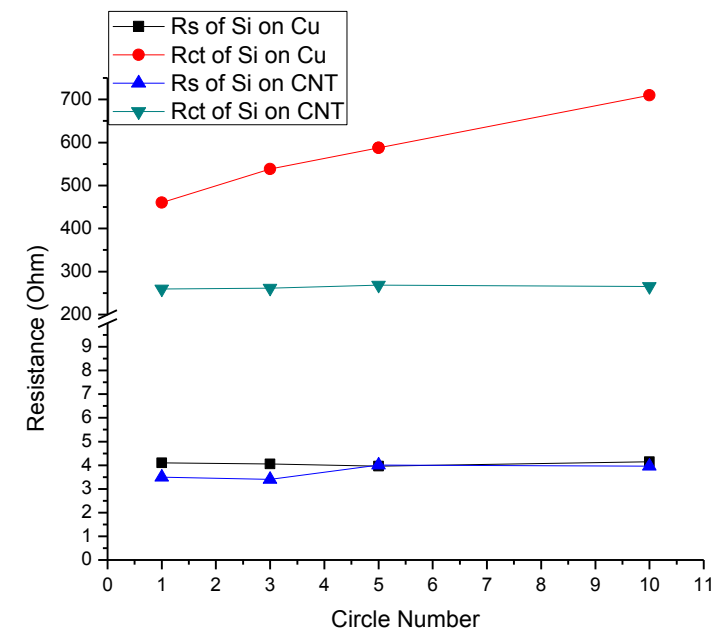
Figure 2.4.3.2 Schematic representatives (cross-section view) of structural evolution of Si films upon charge-discharge cycling. Left column is a Si-Cu sample, fabricated by physically depositing Si film directly on a bare copper current collector; right column represents a Si-SWNT-Cu sample with the SWNT macrofilm as a buffer layer between the deposited Si film and the copper current collector. After 40 charge-discharge cycles, the Si film on the bare copper substrate pulverizes severely into discontinuous particles with various sizes and only minority of the Si particles remain on the current collector. The Si film on the SWNT buffer layer becomes a porous structure but hold tightly onto the SWNT film after getting rid of a few cone-shaped Si pieces. The structural difference of the Si film retention can be attributed to the large-specific-surface-area SWNT buffer layer, which is deformable, stretchable and tolerant to the volumetric expansion and shrinkage of Si films due to lithium ions insertion and extraction, compared to the smooth and rigid copper foil.

To further support the structural evolution model discussed above, electrochemical impedance analysis were conducted on all battery cells from 100 kHz to 10 mHz. The impedance of the anode in the lithium-ion batteries depends strongly on the lithium content inside the electrode materials. To maintain uniformity, electrochemical impedance spectroscopy measurements were carried out on the working electrodes at the de-lithiated state after the 1st, 3rd, 5th, and 10th cycles, respectively. The Nyquist plots obtained are shown in Figs.2.4.3.3a and b, where the high frequency corresponds to the resistance of the electrolytes R_s , the semicircle in the middle frequency range indicates the charge transfer resistance R_{ct} , relating to the charge transfer through the electrode/electrolyte interface and the double layer capacity C_{dl} formed due to the electrostatic charge separation near the electrode/electrolyte interface. Also, the inclined line in the low frequency represents the Warburg impedance W_o , which is related to solid-state diffusion of lithium-ions into the electrode material.

To evaluate effects of different impedance components on the cell degradation along cycling, the electrolyte resistance R_s and the charge transfer resistance R_{ct} were calculated and plotted in Fig. 2.4.3.3c by fitting the Nyquist plots with the corresponding equivalent circuit based on Randles circuit (Fig. 2.4.3.3d) [39]. The electrolyte resistance of both samples is quite comparable within the monitored 10 cycles. However, the charge transfer resistance of the Si-Cu electrode increase significantly during cycling, indicating a larger electrochemical reaction resistance due to the electronic contact loss when the lithiation/delithiation processes take place. This resistance change explains well the rapid degradation of the specific capacity in the cell with Si-Cu. In contrast, stable charge transfer resistance is obtained for the Si-SWNT-Cu electrode during charge-discharge cycles, indicating an excellent structural stability of the electrode

materials as well as a good electronic contact between the active materials and the current collector. These results from impedance analysis are in good agreements with the SEM observations and the charge-discharge cycling performance.





d

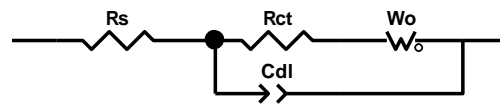


Figure 2.4.3.3 Electrochemical impedance spectroscopy measurements are performed on the cells with Si-Cu sample (a) and Si-CNT-Cu sample (b) separately after the 1st, 3rd, 5th and 10th cycles. The dots in a and b are experimental data, and the lines are curve fitting data with corresponding equivalent circuit in d. Solution Resistance R_c and Charge Transfer Resistance R_{ct} of both Si-Cu and Si-CNT-Cu samples are collected and plotted in c.

2.5 Conclusions

In summary, we present a simple method to fabricate tandem structure of porous Si film on SWNT film to significantly improve the cycling stability of Si film as a promising lithium-ion battery anode material. With new structure using the SWNT film as a buffer layer, reversible specific capacity of Si film retains 2221 mAh g^{-1} after 40 charge-discharge cycles at 0.1 C rate,

which is more than 3 times of the Si film on a bare copper current collector. The unique morphology and structure of the SWNT film not only provide enhanced adhesion between the Si film and the current collector, but also act as a deformable and stretchable substrate to be compliant to the volumetric expansion and shrinkage of the Si film. The facile method and the tandem structure will provide a promising solution for the development of high energy density lithium-ion batteries.

REFERENCE

- 1 B. Scrosati, "Challenge of Portable Power", *Nature*, vol. 373, pp. 557-558, 1995.

- 2 M. K. Aydinol, G. J. Ceder, "First-Principles Prediction of Insertion Potentials in Li-Mn Oxides for Secondary Li Batteries", *Journal of Electrochemical Society*, vol. 144, pp. 3832-3835, 1997.
- 3 M. S. Whittingham, "Electrochemical Energy Storage and Intercalation Chemistry", *Science*, vol. 192, pp. 1126-1127, 1976.
- 4 M. S. Whittingham, A. J. Jacobson, *Intercalation Chemistry*, Academic Press, New York, 1982.
- 5 S. Megahed, B. Scrosati, "Lithium-ion Rechargeable Batteries", *Journal of Power Sources*, vol. 51, pp. 79-104, 1994.
- 6 M. Winter, J. O. Bensenhard, M. E. Spahr, P. Novak, "Insertion Electrode Materials for Rechargeable Lithium Batteries", *Advanced Materials*, vol. 10, pp. 725-763, 1998.
- 7 D. Fauteus, R. Koksang, "Rechargeable Lithium Battery Anode: Alternatives to metallic Lithium", *Journal of Applied Electrochemistry*, vol. 23, pp. 1-10, 1993.
- 8 D. C. S. Souza, V. Pralong, A. J. Jacobson, L. F. Nazar, "A Reversible Solid-State Crystalline Transformation in a Metal Phosphate Induced by Redox Chemistry", *Science*, vol. 14, pp. 2012-2015, 2002.
- 9 E. Kim, D. Son, T. Kim, J. Cho, B. Park, K. S. Ryu, S. H. Chang, "A mesoporous/Crystalline Composite Material Containing Tin Phosphate for Use as the Anode in Lithium-Ion Batteries", *Angewandte Chemie International Edition English*, vol. 43, pp. 5987-5990, 2004.
- 10 Y. Idota, T. Kubota, A. Matsufuji, Y. Maekawa, T. Miyasaka, "Tin-Based Amorphous Oxide: A High-Capacity Lithium-Ion-Storage Material", *Science*, vol. 276, pp. 1395-1397, 1997.
- 11 R. Fong, U. V. Sacken, J. R. Dahn, "Studies of Lithium Intercalation into Carbons Using Nonaqueous Electrochemical Cells", *Journal of Electrochemical Society*, vol. 137, pp. 2009-2013, 1990.
- 12 B. A. Boukamp, G. C. Lesh, R. A. Huggins, "All-solid lithium electrodes with mixed-conductor matrix", *J. Electrochemical Society*, vol. 128, pp. 725-729, 1981.
- 13 J. Graetz, C. C. Ahn, R. Yazami, B. Fultz, "Highly Reversible Lithium Storage in Nanostructured Silicon", *Electrochemical and Solid-State Letters*, vol. 6, pp A 194-197, 2003.

- 14 J. Graetz, C. C. Ahn, R. Yazami, B. Fultz, "Nanocrystalline and Thin Film Germanium Electrodes with High Lithium Capacity and High Rate Capabilities", *Journal of Electrochemical Society*, vol. 151, pp. A698-702, 2004.
- 15 J. P. Maranchi, A. F. Hepp, P. N. Kumta, "High Capacity, Reversible Silicon Thin-Film Anodes for Lithium-Ion Batteries", *Electrochemical and Solid-State Letters*, vol. 6, pp. A198-201, 2003.
- 16 R. Yazami, N. Lebrun, M. Bonneau, M. Molteni, "High Performance LiCoO₂ Positive Electrode Material", *Journal of Power Sources*, vol. 54, pp. 389-392, 1995.
- 17 G. Sandi, R. E. Winans, K. A. Carrado, "New Carbon Electrodes for Secondary Lithium Batteries", *Journal of Electrochemical Society*, vol. 143, pp. L95-L98, 1996.
- 18 T. Ohzuku, Y. Iwakoshi, K. Sawai, "Formation of Lithium-Graphite Intercalation Compounds in Nonaqueous Electrolytes and Their Applications as a Negative Electrode for Lithium Ion (Shuttlecock) Cell", *Journal of Electrochemical Society*, vol. 140, pp. 2490-2498, 1993.
- 19 H. Kim, B. Han, J. Choo, J. Cho, "Three-Dimensional Porous Silicon Particles for Use in High-Performance Lithium Secondary Batteries", *Angewandte Chemie International Edition English*, vol. 120, pp. 10305-10308, 2008.
- 20 M. Holzapfel, H. Buqa, W. Scheifele, P. Novak, F.-M. Petrat, "A New Type of Nano-Sized Silicon/Carbon Composite Electrode for Reversible Lithium Insertion", *Chemical Communication*, pp. 1566-1568, 2005.
- 21 H Ma, F. Y. Cheng, J. Chen, J. Z. Zhao, C. S. Li, Z. L. Tao, J. Liang, "Nest-like Silicon Nanospheres for High-Capacity Lithium Storage", *Advanced Matererials*, vol. 19, pp. 4067-4070, 2007.
- 22 M. H. Park, M. G Kim, J. Joo, K. Kim, J. Kim, S. Ahn, Yi Cui, J. Cho, "Silicon Nanotube Battery Anodes", *Nano Letters*, vol. 9, pp. 3844-3847, 2009.
- 23 L. F. Cui, Y. Yang, C. M. Hsu, Y. Cui, "Carbon-Silicon Core-Shell Nanowires as High Capacity Electrode for Lithium-Ion Batteries", *Nano Letters*, vol. 9, pp. 3370-3374, 2009.
- 24 T. Zhang, H. P. Zhang, L. C. Yang, B. Wang, Y. P. Wu, T. Takamura, "The Structural Evolution and Lithiation Behavior of Vacuum-Deposited

- Si Film with High Reversible Capacity", *Electrochimica Acta*, vol. 53, pp. 5660-5664, 2008.
- 25 L. Y. Beaulieu, K. W. Eberman, R. L. Turner, L. J. Krause, J. R. Dahn, "Colossal Reversible Volume Changes in Lithium Alloys", *Electrochemical and Solid-State Letters*, vol. 4, pp. A137-A140, 2001.
- 26 M. S. Park, G. X. Wang, H. K. Liu, S. X. Dou, "Electrochemical Properties of Si Thin Film Prepared by Pulsed Laser Deposition for Lithium Ion Micro-Batteries ", *Electrochimica Acta*, vol. 51, pp. 5246-5249, 2006.
- 27 T. Moon, C. Kim, B. Park, "Electrochemical Performance of Amorphous-Silicon Thin Films for Lithium Rechargeable Batteries", *Journal of Power Sources*, vol. 155, pp. 391-394, 2006.
- 28 J. T. Yin, M. Wada, K. Yamamoto, Y. Kitano, S. Tanase, T. Sakai, "Micrometer-Scale Amorphous Si Thin-Film Electrodes Fabricated by Electron-Beam Deposition for Li-Ion Batteries", *Journal of Electrochemical Society*, vol. 153, pp. A472-477, 2006.
- 29 Y. L. Kim, Y. K. Sun, S. M. Lee, "Enhanced Electrochemical Performance of Silicon-based Anode Material by Using Current Collector with Modified Surface Morphology", *Electrochimica Acta*, vol. 53, pp. 4500-4504, 2008.
- 30 H. W. Zhu, B. Q. Wei, "Direct Fabrication of Single-Walled Carbon Nanotube Macro-Films on Flexible Substrates", *Chemical Communications*, pp. 3042-3044, 2007.
- 31 A. J. Kinloch, "The Science and Adhesion", *Journal of Materials Science*, vol. 15, pp. 2141-2166, 1980.
- 32 T. Zhang, H. P. Zhang, L. C. Yang, B. Wang, Y. P. Wu, T. Takamura, "The Structural Evolution and Lithiation Behavior of Vacuum-Deposited Si Film with High Reversible Vapacity", *Electrochimica Acta*, vol. 53, pp. 5660-5664, 2008.
- 33 A. M. Wilson, J. R. Dahn, "Lithium Insertion in Carbons Containing Nanodispersed Silicon", *Journal of Electrochemical Society*, vol. 142, pp. 326-332, 1995.
- 34 S. H. Ng, J. Z. Wang, D. Wexler, K. Konstantinov, Z. P. Guo, H. K. Liu, "Highly Reversible Lithium Storage in Spheroidal Carbon-Coated Silicon Nanocomposites as Anodes for Lithium-Ion Batteries",

- Angewandte Chemie International Edition English, vol. 45, pp. 6896-6899, 2006.
- 35 Y. Liu, Z. Y. Wen, X. Y. Wang, X. L. Yang, A. Hirano, N. Imanishi, Y. Takeda, "Improvement of Cycling Stability of Si Anode by Mechanochemical Reduction and Carbon Coating", *Journal of Power Sources*, vol. 189, pp. 480-484, 2009.
 - 36 R. Teki, M. K. Datta, R. Krishnan, T. C. Parker, T. M. Lu, P. N. Kumta, N. Koratkar, "Nanostructured Silicon Anodes for Lithium Ion Rechargeable Batteries", *Small*, vol. 5, pp. 2236-2242, 2009.
 - 37 B. Laik, L. Eude, J. P. Pereira-Ramos, C. S. Cojocar, D. Pribat, E. Rouviere, "Silicon Nanowires as Negative Electrode for Lithium-Ion Microbatteries", *Electrochimica Acta*, vol. 53, pp. 5528-5532, 2008.
 - 38 C. K. Chan, H. L. Peng, G. Liu, K. McIlwrath, X. F. Zhang, R. A. Huggins, Y. Cui, "High Performance Lithium Battery Anodes Using Silicon Nanowires", *Nature Nanotechnology*, vol. 3, pp. 31-35, 2008.
 - 39 J. E. B. Randles, "Kinetics of Rapid Electrode Reactions", *Discussions of the Faraday Society*, vol. 1, pp. 11-19, 1947.

Chapter 3

STRETCHABLE SUPERCAPACITORS BASED ON BUCKLED SINGLE-WALLED CARBON NANOTUBE MACRO-FILMS

3.1 Introduction to Supercapacitor

3.1.1 Brief History of Supercapacitor

The first patent on supercapacitor was issued to Becker at General Electric Corporation in 1957 [1] where, a capacitor based on high surface area porous carbon materials was described. The first attempt to commercialize supercapacitors with high surface area carbon materials and tetraalkylammonium salt electrolyte was done by Sohio in 1969 [2]. In the following decades, Conway and coworkers made a significant contribution to the supercapacitor research based on RuO_2 [3]. By early 1990's, supercapacitors received much attention in the context of hybrid electric vehicles. A large number of supercapacitor patent have been granted as cited by Sarangapani in 1996 [4]. These studies triggered U. S. Department of Energy to initiate short term and long term supercapacitor development programs.

In recent years, supercapacitors have attracted great interest, due to their high power and energy densities compared with lithium-ion batteries and conventional dielectric capacitors, respectively. The most active research in supercapacitors is the development of new electrode materials to fulfill the high power and energy densities. Recently, carbon nanotubes (CNTs) have been studied as good candidates for electrode materials [5], because of several advantages,

including high surface area for storing charge and more efficient interactions with electrolyte, nanoscale dimensions for miniaturization of capacitor devices in terms of both size and weight, and excellent electrical conductivity for the possible removal of any current collectors.

3.1.2 Supercapacitor Operation Principle

Electrochemical Double-layer Capacitors (EDLCs) consist of two high surface area porous electrode materials coated on current collectors and placed parallel to each other with an electrolyte soaked separator in between them as shown in Figure 3.1.2.1. The energy storage in the electrochemical capacitor takes place in an electrical double layer that is formed at the porous electrode/electrolyte interface. Positive (cations) and negative (anions) ionic charges within the electrolyte accumulate at the surface of the solid electrode and compensate for the electronic charge at the electrode surface. The thickness of the double layer depends on the concentration of the electrolyte and on the size of the ions and is in the order of 2-10 Å for concentration electrolytes.

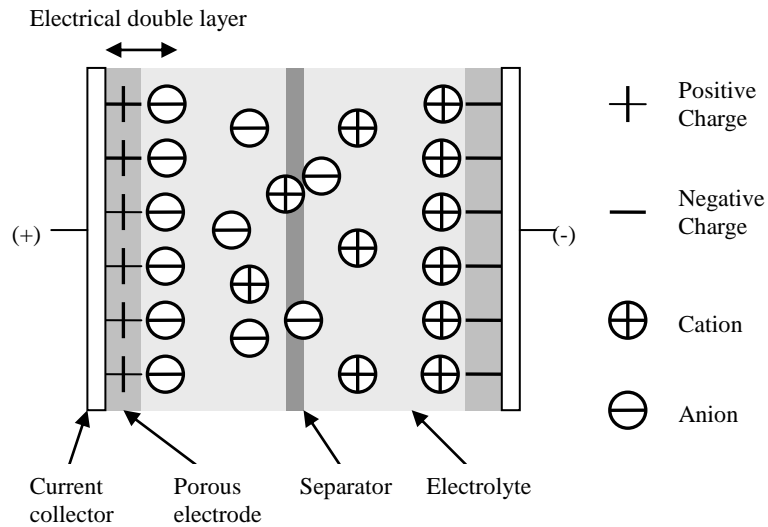


Figure 3.1.2.1 Schematic representative of electrochemical double layer capacitor

In a conventional capacitor with two similar parallel plates each with area A and separated by a distance d with a dielectric material of permittivity ϵ , the capacitance is given by $C = \epsilon A/d$. Such a capacitor gives a value of capacitance in the range of pF or μF . In case of the EDLC, since the porous electrode material have very high specific surface area and the double layer width d is in the order of few \AA , a very large capacitance value will be obtained from the equation mentioned above. Depending on the type of high surface area material being used, the capacitance in the EDLC could vary from milli-Farads to several tens of Farads.

The charging and discharging in the EDLC involves no chemical phase and

composition changes. Only electrons move to and from the electrode surfaces through the external circuit, and cations and anions of the electrolyte transport within the electrolyte solution to the charged interface. Such capacitors have very high degree of recyclability on the order of 10^5 - 10^6 times.

3.2 Significance

Progress in electronics is driven mainly by efforts to increase circuit operating speeds and integration densities, to reduce the power consumption of circuits, and, for display systems, to enable large area coverage. A more recent direction seeking to develop methods and materials that enable high-performance circuit to be formed on un-conventional substrates with unusual form factors, namely flexible and stretchable electronics that have attracted considerable attention from scientific and technological communities, has opened the door to many important applications that current, rigid electronics cannot achieve [6]. Stretchable electronic devices, such as p-n diodes [7], photovoltaic devices [8], transistors [9] have been fabricated using buckled single crystal (e.g., Si, GaAs) thin films supported by elastomeric substrates. In order to accommodate the needs of the flexible and stretchable electronics, power source devices, as indispensable components in all electronics, must also be flexible and stretchable in addition to their high energy and power density, light weight, miniaturization in size, and safety requirements. We fabricated reversibly stretchable supercapacitors using buckled single-walled carbon nanotube (SWNT) macro-films as the electrodes, which have controllable wavy geometries and show extremely high mechanical stretchability (up to 30%) with the utility of polydimethylsiloxane (PDMS) as the elastomeric substrates. The stretchable supercapacitors exhibit very stable capacitance under cyclic stretching and releasing, and comparable energy and power densities with those using pristine SWNT macro-films as electrodes. Without intolerant variation of their electrochemical performances while

stretching, the stretchable supercapacitors are therefore found to be excellent candidates for the power sources of stretchable electronics and other applications in which large mechanical deformation is anticipated.

3.3 Experimental Section

3.3.1 Preparation of PDMS Substrate

PDMS was prepared by mixing silicone elastomer base and curing agent (Sylgard 184, Dow Corning) at the ratio of 10:1 by weight. Rectangular slabs of 1.5 cm by 6 cm were cut from the polymerized PDMS. Rinse the slab with isopropyl alcohol (IPA) to remove contaminations and dry it. A custom made stage was utilized to stretch the PDMS to specific strain levels (Figure 3.3.1.1). The pre-strained PDMS substrate was subjected to a flood exposure by a UV light (low pressure mercury lamp, BHK) for 150 seconds. The 185 nm radiations produce ozone, while the 254 nm radiations dissociate the ozone to O_2 and atomic oxygen (O) to form a chemically activated surface on PDMS.

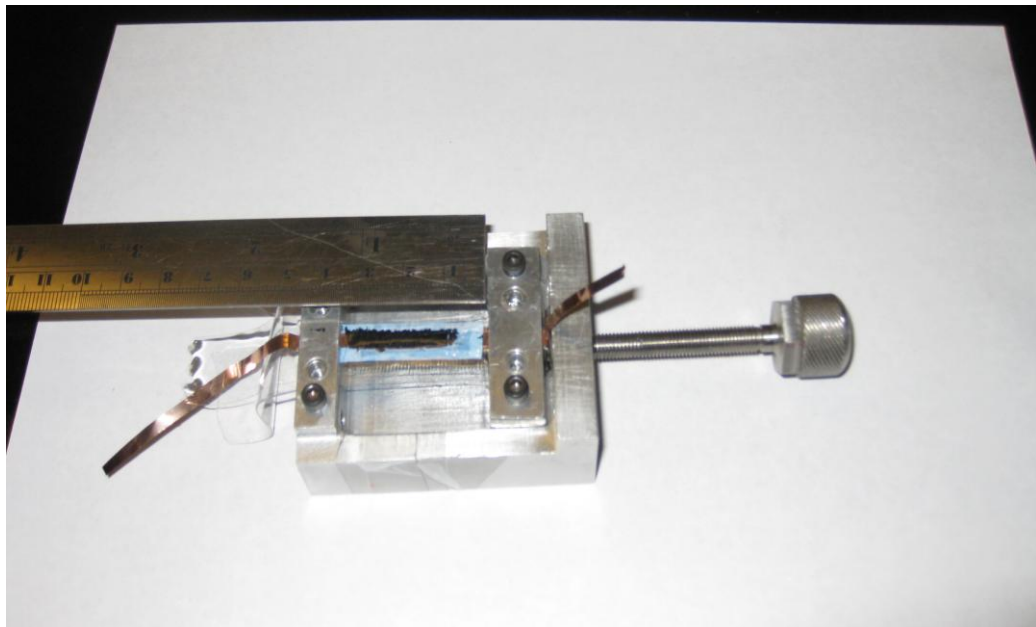


Figure 3.3.1.1 The two-electrode supercapacitor setup using a custom made stage favorable for stretching the supercapacitor to a specific length.

3.3.2 Fabrication of Buckled Single-Walled Nanotube Macro-Film on Elastomeric PDMS Substrate

The stretchable supercapacitor consists of two periodically buckled single-walled carbon nanotubes (SWNT) macro-films as stretchable electrodes, organic electrolyte and a polymeric separator. The preparation of the buckled SWNT macro-films is the key component for stretchable supercapacitors. The synthesis of high-quality functionalized SWNT macro-film is introduced in chapter 1. In brief, the synthesis of the SWNT films involves a simple floating CVD method using ferrocene as carbon feedstock/catalyst and sulfur as an additive to promote SWNT growth to a high percentage. The SWNT films obtained from CVD were purified by first heating the films in air up to 450°C to remove amorphous carbon and then treated in 9 M HCl solution to remove the iron catalyst particles. The purified SWNT macro-film significantly increases chemically activated functional groups (e.g. O=C–OH) on SWNTs [10].

The purified SWNT macro-film was then buckled by following the steps shown in Fig. 3.3.2.1. The procedure introduced here (steps i and ii in Fig. 3.3.2.1) involved uniaxially pre-

stretching an elastomeric substrate of poly(dimethylsiloxane) (PDMS) slab ($\epsilon_{pre} = \Delta L/L$ for length changed from L to $L+\Delta L$) followed by UV treatment to form hydrophilic surface. The exposure of ultraviolet (UV) light introduces atomic oxygen (O), that reacts with PDMS thus to change the hydrophobic surface (dominated by $-\text{OSi}(\text{CH}_3)_2\text{O}-$ groups) to hydrophilic surface (terminated with $-\text{OSi}(\text{OH})_{4-n}$ functionalities) [11]. The formed hydrophilic surface of PDMS is able to form strong chemical bonding between $-\text{OH}$ groups on SWNT films through condensation reactions. The purified SWNT macro-film with extensive $-\text{OH}$ groups was laminated with the pre-strained, UV-treated PDMS substrate along the direction of the pre-strain on a custom made stage (step iii) to form covalent bonds ($-\text{C}-\text{O}-\text{Si}-$) through condensation reaction. Releasing the pre-strain in PDMS substrate led to the spontaneous formation of buckled patterns due to mechanical competition between the SWNT macro-film and PDMS substrate (step iv).

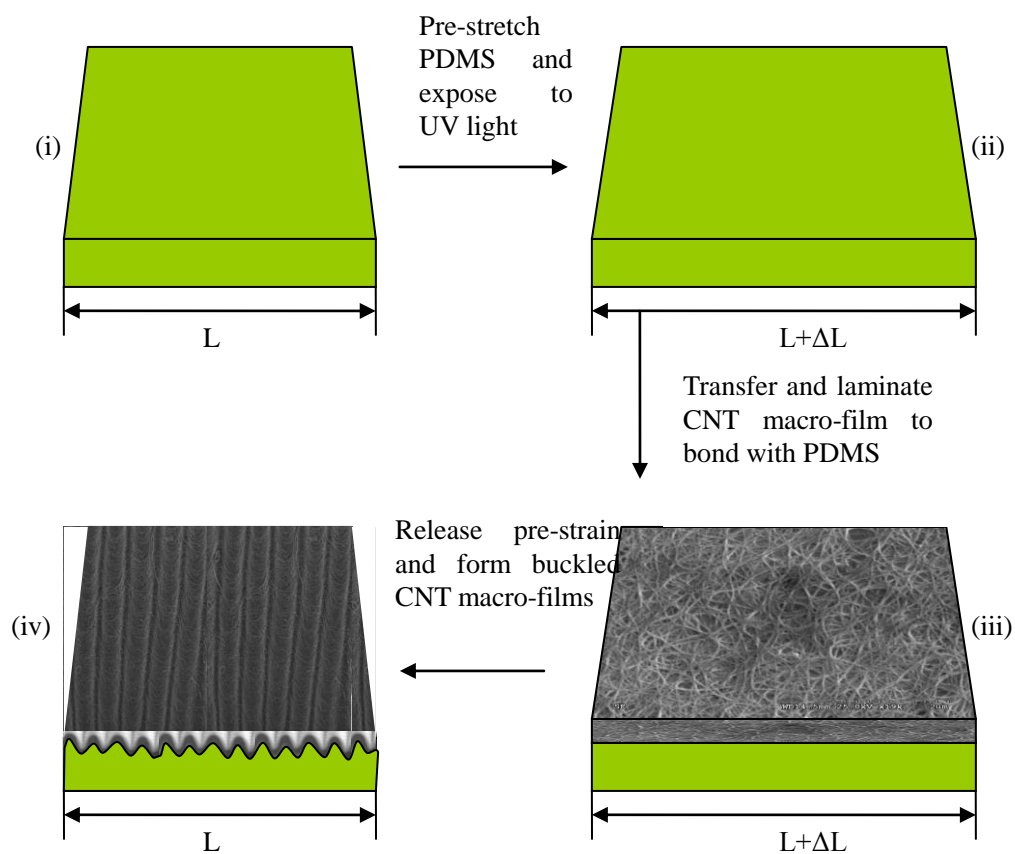


Figure 3.3.2.1 Fabrication steps of a buckled SWNT macro-film on elastomeric PDMS substrate.

3.3.3 Supercapacitor Assembly and Electrochemical Measurements

The supercapacitor was assembled as a two-electrode system. A 1M tetraethylammonium tetrafluoroborate (TEABF₄) dissolved in propylene carbonate (PC) was used as the electrolyte. Two PDMS sheets with buckled SWNT films were pressed together separated by a filter paper soaked in the electrolyte. Two thin copper strips were used as current collectors. The assembly and all measurements were carried out in a Glove box (Unilab, MBraun) filled with

argon. Cyclic voltammetry (CV) was carried out from -1.5 V to +1.5 V using an Autolab Potentiostat/Galvanostat. Galvanostatic charge-discharge measurements were tested with a four channel Arbin system. First, all the electrochemical measurements on the supercapacitor with buckled SWNT film electrodes were measured in un-stretched condition. Then, by using the custom made stage, 30% tensile strain was applied to the stretchable supercapacitor. The measurements on the stretched supercapacitor were carried out. The specific capacitance was calculated as

$$C=2I \cdot \Delta t / (m \cdot \Delta V) \quad 3.1$$

Where I is the applied current and m is the average mass of the two electrodes. The energy and power density were calculated by conducting galvanostatic charge-discharge cycling with different constants current densities.

3.4 Results and Discussion

To demonstrate the feasibility of the stretchable supercapacitors with almost constant electrochemical performances (capacitance, energy densities and cycling stability), stretchable supercapacitors with the buckled SWNT macro-films as electrodes were assembled and their electrochemical performance were studied. In the following tests, the buckled SWNT macro-films in supercapacitors were formed by releasing the PDMS substrates with 30% pre-strain and the pristine supercapacitor electrodes were formed by laminating PDMS and SWNT films in free condition. The electrochemical characterizations were conducted with the stretchable supercapacitors at both 0% applied stain and 30% applied strain. The same measurements are carried out with the pristine supercapacitor for comparison. Figures 3.4.1 shows the cyclic

voltammograms (CVs) of the stretchable supercapacitor subjected to different applied strain. The CVs retained rectangular shape with ideal capacitive behavior at different applied strain. Besides, no significant change was observed in the CVs of the stretchable supercapacitors with 0 and 30% applied strains. The CVs results reveal that the energy density and capacitance of the stretchable supercapacitor were almost invariant with up to 30% applied stain.

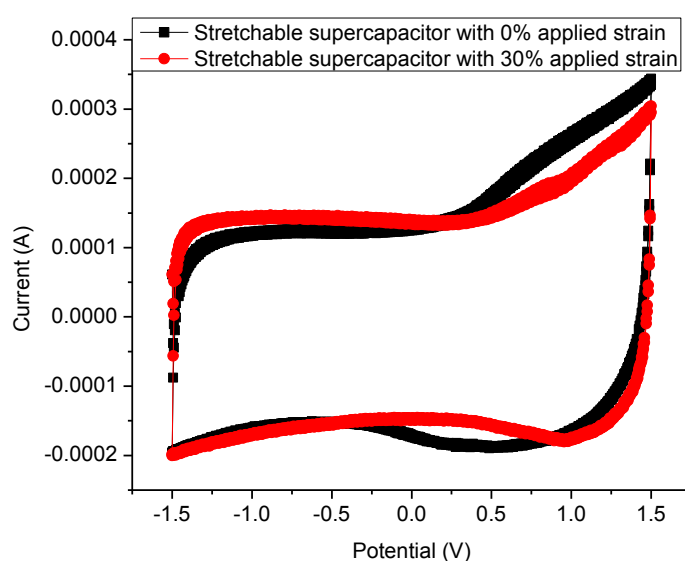
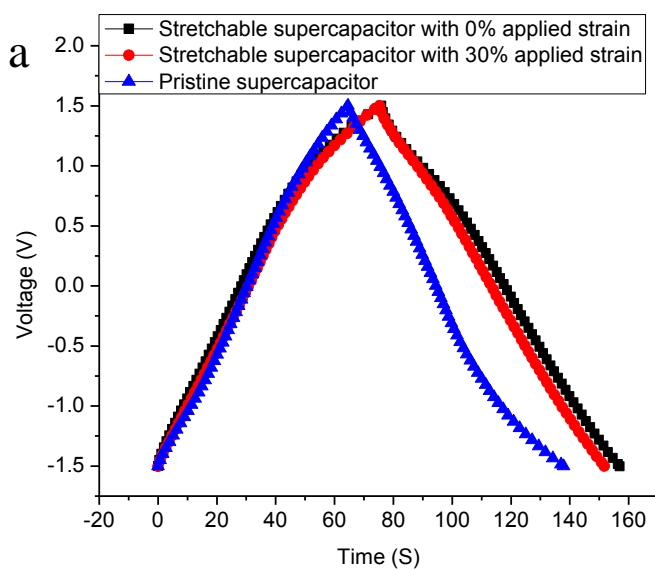


Figure 3.4.1 Cyclic voltammograms of the stretchable supercapacitor measured at 0% and 30% applied strain.

The cycling stability of the stretchable supercapacitors subjected to applied strains along with the pristine supercapacitor illustrated by galvanostatic charge-discharge with a constant current density of 1 A g^{-1} up to 1000 cycles (Fig. 3.4.2). The initial specific capacitances calculated from the discharge slopes (Fig. 3.4.2 a) were 54 F g^{-1} for the stretchable supercapacitor with 0%

applied strain and 52 F g^{-1} for that subject to 30% applied strain. These values are very comparable to the specific capacitance of the pristine supercapacitor, which is 50 F g^{-1} . Remarkably, the specific capacitances of stretchable supercapacitors with or without applied strain experienced minor variance even up to 200 charge-discharge cycles (Fig. 3.4.2 b), which concludes excellent electrochemical stability. All these results demonstrate that the stretchable supercapacitor we assemble here can be stretched up to 30% without changing its electrochemical performance.



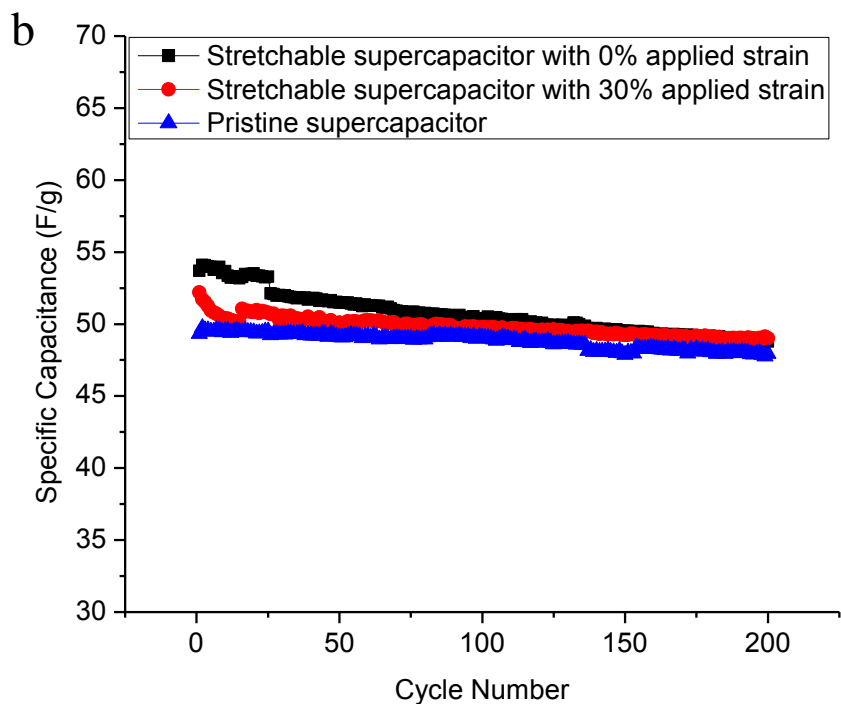


Figure 3.4.2 Galvanostatic charge-discharge measurements of stretchable supercapacitor and pristine supercapacitor. (a) illustrates galvanostatic charge-discharge in a constant current density of 1A g^{-1} with stretchable supercapacitor subjected to different applied strain and pristine supercapacitor. The cycling stability of both supercapacitors is shown in (b).

3.5 Conclusions

In summary, this study exhibits a promising approach to develop stretchable supercapacitors based on buckled SWNT macro-films as electrodes, for unusual power source applications. The stretchability depends on the level of pre-stain applied on the PDMS substrate, which could be as high as 30%. The electrochemical performance remains invariant during

mechanical stretch. This stretchable supercapacitor reported here just enlightens a broad area of stretchable energy storage devices, which are naturally compatible with the developed stretchable electronics.

REFERENCE

- 1 H. E. Becker, U. S. Patent, no. 2800616, 1957
- 2 D. I. Boos, U. S. Patent, no. 3536963, 1970.

- 3 B. E. Conway, "Transition from Supercapacitor to Battery Behavior in Electrochemical Energy Storage", *Journal of Electrochemical Society*, vol. 138, pp. 1539-1548, 1991.
- 4 S. Sarangapani, B. V. Tilak, C. P. Chen, "Materials for Electrochemical Capacitors", *Journal of Electrochemical Society*, vol. 143, pp. 3791-3799, 1996.
- 5 C. M. Niu, E. K. Sichel, R. Hock, D. Moy, H. Tennent, "High power electrochemical capacitors based on carbon nanotube electrodes", *Applied Physics Letters*, vol. 70, pp. 1480-1482, 1997.
- 6 H. Klauk, "Device physics: nanowires display of potential", *Nature*, vol. 451, pp. 533-534, 2008
- 7 D.Y. Khang, H. Q. Jiang, Y. G. Huang, J. A. Rogers, "A stretchable form of single-crystal silicon for high-performance electronics on rubber substrates", *Science*, vol. 311, pp. 208-212, 2006.
- 8 Y. G. Sun, W. M. Choi, H. Q. Jiang, Y. G. Huang, J. A. Rogers, "Controlled Buckling of Semiconductor nanoribbons for stretchable electronics", *Nature Nanotechnology*, vol. 1, pp. 201-207, 2006.
- 9 D. H. Kim, J. H. Ahn, W. M. Choi, H. S. Kim, T. H. Kim, J. Z. Song, Y. G. Huang, Z. J. Liu, C. Liu, J. A. Rogers, "Stretchable and foldable silicon integrated circuits", *Science*, vol. 320, pp. 507-511, 2008.
- 10 H. W. Zhu, B. Q. Wei, "Direct fabrication of single-walled carbon nanotube macro-films on flexible substrates", *Chemical Communications*, vol. 29, pp. 3042-3044, 2007.
- 11 M. Ouyang, C. Yuan, R. J. Muisener, A. Boulares, J. T. Koberstein, "Conversion of some siloxane polymers to silicon oxide by UV/ozone photochemical processes", *Chemistry of Materials*, vol. 12, pp. 1591-1596, 2000.

Chapter 4

CONCLUSIONS, PUBLICATIONS AND FUTRUE WORK

4.1 Conclusions

Applications of SWCNT film in various electrochemical energy storage devices are demonstrated in this thesis. In Chapter 2, a simple method to fabricate tandem structure of porous Si film on SWNT film to significantly improve cycling stability of Si film as lithium-ion battery anode material was demonstrated. With the new structure, both reversible specific capacity and cycling stability are improved. Reversible specific capacity of Si film retains 2221 mAh g^{-1} after 40 charge-discharge cycles at 0.1C rate, more than 3 times that on regular copper current collector. The unique morphology of SWNT film was found to be responsible for the enhanced reversible specific capacity. With assistance of SWNT film, Si film is formed of cone-shaped lattice during physical deposition, some of which could be easily removed to release internal stress to maintain stability of Si film during charge-discharge cycling and the majority of Si could be held by the deformable, stretchable SWNT film during volume expansion and shrinkage.

SWNT macro-films also exhibits a promising application in stretchable supercapacitors based on buckled SWNT marco-film electrodes for unusual power source applications in Chapter 3. The stretchability depends on the level of pre-stain applied on the PDMS substrate, which could be as high as 30%. The electrochemical performance remains unchanged during mechanical stretch. This stretchable supercapacitor just enlightens a broad area of

stretchable energy storage devices, which are naturally compatible with the developed stretchable electronics.

4.2 Publications

- [1] C. J. Yu, C. Masarapu, J. P. Rong, B. Q. Wei, H. Q. Jiang, “Stretchable Supercapacitors Based on Buckled Single-Walled Carbon-Nanotube Macrofilms”, *Advanced Materials*, vol. 21, pp. 4793-4797, 2009.
- [2] J. P. Rong, C. Masarapu, J. Ni, Z. J. Zhang, B. Q. Wei, “Tandem Structure of Porous Silicon Film on Single-Walled Carbon Nanotube Macrofilms for Lithium-Ion Battery Applications”, submitted.

4.3 Future Work

Although SWNT macro-films showed promising applications in improving lithium-ion battery electrode specific capacity and cycling stability, as well as novel electrode materials in stretchable supercapacitors. There is still great progress need to make to make it applicable in commercial products.

One limitation of SWNT macro-film applications is the effective synthesis technique to make it in larger size and in continuous operation. Besides, to fabricate a better stretchable energy storage device, each component needs to be stretchable. SWNT macro-films and PDMS are both stretchable working as electrode material and substrate separately. Separator, usually made of porous polyethylene membrane or glass fiber filter paper, is also need to find other elastomeric materials as substitute.